[Supplementary Materials]

A typical post-war workshop: Insights into Simon Hantaï's oil paint palette

Lauren Dalecky, Ilaria Bonaduce, Étienne Anheim, Jacopo La Nasa, Maëva L'Héronde, Clément Morel, Emilio Catelli, Silvia Prati, Zelan Li, Lucile Beck, Ingrid Caffy, Emmanuelle Delqué-Količ, Aurélia Chevalier, Loïc Bertrand

Contents

S1 Acronyms used in this work

A/P	Azelaic over palmitic acid ratio
AsB	Angle selective backscatter
AMS	Accelerator mass spectrometry
BF	Bright field
BSTFA	N,O-Bis(trimethylsilyl)trifluoro acetamide
C14	Carbon 14
Cbx	Carboxylate
CS	Cross-section
DAG	Diacylglycerol
DF	Dark field
EIC	Extracted ion chromatogram
FFA	Free fatty acid
FIA-MS	Flow injection analysis – mass spectrometry
FMS	Free metal soaps
Frs	Francs
FT-IR	Fourier-transform – infrared spectroscopy
GC-MS	Gas chromatography–mass spectrometry
GJ	2015 sample in glass jar
HDMS	Hexamethyldisilazane (hydrophobic substance)
HPLC	High-performance liquid chromatography
HPLC-ESI-Q-Tof	High-performance liquid chromatography – electrospray ionization – quadrupole – time of flight
HPLC-MS	High-performance liquid chromatography – mass spectrometry
ICDD	International Centre for Diffraction Data
IS	Internal standard
LOD	Limit of detection
LOQ	Limit of quantitation
MS	Metal soaps
M/S	Myristic over stearic acid ratio
Ox	Oxalate
O/S	Oleic over stearic acid ratio
PF	2015 sample in plastic film
pMC	Percent modern carbon
PN	Polymeric network
P/S	Palmitic over stearic acid ratio
PUFA	Polyunsaturated fatty acid
Py-GC-MS	Pyrolysis – gas chromatography – mass spectrometry
S.A.R.L.	Société à responsabilité limitée
SEM-EDX	Scanning electron microscope – energy dispersive X-ray spectrometry
SR-μ-XRD	Synchrotron radiation micro X-ray diffraction
TAG	Triacylglycerol
TMS	Trimethylsilyl
XRD	X-ray diffraction

S2 Additional historical information about the painter Simon Hantaï

S2.1 Artistic journey

Simon Hantaï (1922–2008) was an influential painter in the postwar era of Paris. Hantaï's artistic influences included, notably, Jackson Pollock's for his gesturality [1] and Henri Matisse's for his use of color. The latter had been a reference for Hantaï as early as his studies in Budapest in the 1940s [2]. He arrived in Paris in 1948, and eventually, joined the surrealist group under André Breton, with his first public exhibition in 1952. Hantaï eventually broke away from the group in 1955 [3], and would quickly start playing with gestural techniques and the all-over method, developing his own artistic process and practice. His most famous works were made by his original technique that he designated as *pliage* or "folding as a method", where his process was to prepare large pieces of canvas, fold the canvas in ordered or more random patterns, apply colored paint, and unfold to reveal the patterns of paint [4]. Hantaï's describes his practice as the "crab walk", in which instead of progressing through his method in a linear manner, his process through each period is made unique by him moving in many directions, including backwards, by creating, modifying and recreating works [5, p. 29].

Hantaï's experimentation with pictorial techniques (scraping, rubbing, collage, decalcomania, and painting on printed newspaper, texts or photographs from magazines or advertisements, etc.) is observed in *le Grand livre des petites peintures* ("The big book of small paintings", 1949–1963), with his earliest "pliage" dated 1950 [6]. However, it was not until the 1960s when he would exhibit his first *pliage* series, which he would spend over three decades pursuing, practicing, perfecting and imperfecting, creating many series — *Mariales* (1960–1961), *Catamurons* (1963–1965), *Panses Saucisses* (1964–1967), *Meuns* (1966–1968), and *Études* (1968–1971), *Aquarelles* (1971–1972), *Blancs* (1973–1975), *Tabulas* (1973–1976), second *Tabulas* (1980–1981) and *Tabulas Lilas* (1982) [6]. After an exhibition in 1982, Hantaï had a period called "artistic suicide" where he stopped painting and displaying his works publicly for a number of years to demonstrate his discontent with the institutions [7, 8], though he continued to rework old pieces. He created what is referred to as the "last studio", *Pliages interminables par réductions successives*, which comprises of "drip-folds", "reframed paintings", "prepared folds" and "unfolded forms" of the *Tabulas* and *Blancs* [6]. He also modernized the series *Tabulas* by transforming them into new works by cutting the large canvases into separate pieces, known as the *Laissées* (1994–1995), as a way to dissociate these works from the institutions that he was against [8]. The exhibition of his "last studio" series in 1998 would end his silence from the public eye. He continued his development as an artist in his later years by exploring outside of painting: photography, digital scanning and silkscreen printing of his paintings, *Sérigraphies* (1996–1999) and *Suaires, h.b.l.* (2000–2001), and also, conservation through a collaboration with the contemporary art restorer Aurélia Chevalier, who developed the "marouflage Hantaï" [9] to increase the resistance of his paintings to time, give a sense of strength to his large-format paintings so that one had the impression that "the wall carries the canvas", as well as give vibrancy to the color. Hantaï worked on his artworks until his passing in September 2008 in Paris [6].

S2.2 Description of Hantaï's atelier

In *L'Étoilement*, the philosopher Georges Didi-Huberman [9] describes Hantaï's atelier:

> His space whispers something for him: there is no furniture (only a large white table and only two chairs). The walls disappear behind large paintings piled on top of each other,

> spilling over the sides, already leafing through our colorful sensation, invading our gaze with all these exploded planes. An impression of multiple flashes and starbursts: rifts of color, movements, embraces, holes, welts. At the same time, embarrassed silence. Embarrassment and amazement mixed together. One doesn't know where to look, or where to start. Another thing increases my confusion: there is here a kind of inversion of my familiar spaces, which are inhabited by libraries. Not a book on the wall, only these starry colors. But on the floor, hundreds, thousands of books in heaps: mountains, valleys, landscapes of books (I will verify a little later that Hantaï knows every place, every corner of this maquis). Poetry and philosophy make the floor of his house.

Original text in French:

> Son espace murmure quelque chose pour lui : il n'y a pas de meuble (seulement une grande table blanche et seulement deux chaises). Les murs disparaissent derrière de grands tableaux empilés les uns sur les autres, débordant sur les côtés, feuilletant déjà notre sensation colorée, envahissant notre regard de tous ces pans explosés. Impression d'éclairs et d'étoilements multiples : failles de couleurs, mouvements, embrassements, trouées, zébrures. En même temps, silence embarrassé. Gêne et sidération mêlées. On ne sait où poser les yeux, ni par quoi commencer. Autre chose accroît mon trouble : il y a ici comme une inversion de mes espaces familiers, qu'habitent des bibliothèques. Pas un livre au mur, seulement ces couleurs étoilées. Mais, sur le sol, des centaines, des milliers de livres en tas : des montagnes, des vallées, des paysages de livres (je vérifierai un peu plus tard que Hantaï connaît chaque place, chaque recoin de ce maquis). Poésie et philosophie font le sol de sa maison. (Didi-Huberman [9, p. 17])

S3 Detailed description of the materials

The paint manufacturers discussed in this article began their history as small businesses composed of a few color men, who were prominent in the late 19th and early 20th centuries. In the postwar period, there was a transition from these figures to larger industries. The evolution of many manufacturers within a few decades resulted in the loss of many records [10]. The study of Hantaï's collection is particularly valuable for identifying the constituent or expected materials in the works of artists working in Paris in the second half of the 20th century, and providing insights on the evolution of paint formulation.

S3.1 Lefebvre-Foinet tubes

Hantaï's collection is representatives of the postwar period. Lefebvre-Foinet paints, constituting the main part of our corpus, have been used by many artists who worked in Paris during the period, including Henri Matisse, Alberto Giacometti, Fernand Léger, Pierre Soulages, Joan Mitchell, Jean-Paul Riopelle [11] and Piet Mondrian [12]. Lefebvre-Foinet was founded in the 1880s by Paul Foinet, who went door-to-door to artist's studios supplying them with hand-ground colors, hand-primed canvases and pincers. A boutique opened in 1902 by Lucien Lefebvre, Foinet's son-in-law, in the Montparnasse neighborhood in the sixth district of Paris [13]. In the mid-20th century, Maurice (Lucien's son) Lefebvre-Foinet was in close contact with many artists who bought their supplies from him and had many artworks dedicated to the family [14]. The store eventually closed in 1996 [15]. Riopelle described its colors as “unique” [11] and Mondrian raved about its wide selection of colors in saying, “you’ll find every shade of red, blue and yellow” [12]. Soulages cited the types of oils used by Lefebvre-Foinet as Bombay linseed oil and La Plata linseed oil; he mentioned that the oils were of a decent quality compared to other paint makers of the time period, so many artists were using them in the 1950s [16].

Lefebvre-Foinet tubes are labeled as followed: (1) “LUCIEN LEFEBVRE-FOINET” in a bold sans serif font, (2) S.A.R.L. capital value, (3) address, (4) paint designation in French, and (5) paint designation Differences between the labels were noted in the font. They were categorized into four groups, described in the Table S3.1.

Table S3.1: Text written on the labels of the four groups of Lefebvre-Foinet tubes.

	1	**2**	**3**	**4**
Tubes	LF-O-CdRO, LF-O-CdRP, LF-O-CdRV, LF-O-CdYO	LF-O-CdYM, LF-O-PGD4	LF-O-CdR	LF-O-PGD16, LF-O-CB, LF-O-MB, LF-O-UB
S.A.R.L.	S.A.R.L. au capital de 1.700.000 Frs	N/A	S.A.R.L. au capital de 50.000 F	S.A.R.L. au capital de 17.000 Frs
Address	19, RUE VAVIN & 2, RUE BRÉA, PARIS, serif	19, RUE VAVIN & 2, RUE BRÉA, PARIS, serif	19, RUE VAVIN & 2, RUE BRÉA, PARIS, sans serif	2, RUE BRÉA, PARIS & 19, RUE VAVIN, sans serif
Pigment font FR	Bold, sans serif	Bold, sans serif	Bold, sans serif, small	Bold, sans serif
Pigment font EN	Italic, serif	Italic, serif	Bold, sans serif, small	Bold, sans serif, small
Color of twist cap	Black	Black	Red	Black

We detail below the condition of each of the tubes:

LF-O-CdR This tube was stored in a cardboard box, and appears to be in good condition and unused. Some degradation is seen by brown material under the red twist cap. The tube is reflective but has been slightly dulled, by small black dots on the tube and the surface of the tube appears slightly rough. The strip of color painted over the label is bright red. The label is fully intact and slightly tanned from its original white. The typeface for the label of this tube is unique to this tube, in smaller text in comparison to the others, and both the paint name in French and English are in bold. It is the only tube with an S.A.R.L. capital of 50.000 Frs.

LF-O-CdRO The tube appears to have been used, there is the red-orange paint drips on the black twist cap. The tube is reflective, with black streaks running down the tube. There are drips of material running down from the top of the tube to the bottom. This appeared to remove some of the red-orange paint above the label and caused some degradation of the paint label. The bottom of the tube is also degraded significantly with black material at the seam of the tube. The label is yellow-brown with a type face bold for the paint name in French and italicized for the paint name in English (same as LF-O-CdRP, LF-O-CdRV). The S.A.R.L. capital value is 1.700.000 Frs.

LF-O-CdRP The tube has a black twist cap, and if ever used appears to be sealed tightly, as there is no degrading material under the black twist cap. Some dirt is present around the cap and over the red-purple paint above the label. The tube has some black spotting and streaking the length of the tube. Also, black degradation material is present along the seam at the bottom of the tube. The label is browned and has the same format and S.A.R.L. value as LF-CdRO.

LF-O-CdRV This tube was stored in a cardboard box, similar to that of Cadmium Red, and it appears to be in good condition and unused. Also, like the Cadmium Red sample, this is the only other tube with a colored twist cap, in this case red. The tube is reflective, but has been dulled by black spotting on the surface, which appears rough. The label has the same format and S.A.R.L. value as LF-CdRO.

LF-O-CdYO The tube appears to have been used as it is wrinkled as if squeezed. Around the black twist cap is dust and webs, and the orange paint strip above the label has almost entirely fallen off. There are black streaks running down the tube as well as some spotting. The bottom of the tube has some altered material that is more brown-orange, in comparison to the previously described degradation material that was black. The tube has no visible degraded paint material under the black twist cap. The label has darkened slightly in color and has the same format and S.A.R.L. value as LF-CdRO, except the text for the paint name in French is in all capital letters.

LF-O-CdYM The tube appears to have been used as it is wrinkled as if squeezed and is even covered in spots of other paint colors – green, black, and yellow – along with black streaking down. the tube. The tube is sealed with a black twist cap and degraded yellow paint is seen under. A stripe of yellow paint above the label is heterogeneous in color with light yellow and dark yellow drips. The paint label is a tan-yellow and has the same format as LF-CdRO, except the text for the paint name in French is in all lowercase letters and this label has no S.A.R.L. capital value visibly written on the tube.

LF-O-PGD4 The tube is wrinkled and appears to have been used. There is green paint visible under the black twist cap. The green paint above the label is heterogeneously painted and is slightly chipped. Black streaks run down the entirety of the tube, with some black spotting mostly present under the label. At the bottom of the tube, a tan, grainy material is on the tube, and there is some dark green paint color or black material near the seam. The color of the label is white and appears in good condition, has the same format as LF-CdYM, except the text is not all lowercase. Like LF-O-CdYM, there is no S.A.R.L. capital value visibly written on the tube.

LF-O-PGD16 The tube appears brand new, in almost perfect condition and unused. The tube itself is lustrous and appears smooth with very minimal degradation. The only appearance of aging is a few black streaks running down from the label. Above the label, the green paint is a homogeneous layer. The label is white and in a modern typeface with an S.A.R.L. capital of 17.000 Frs. The address indicated changes from “19, R. VAVIN & 2, R. BRÉA, PARIS” to “2, R. BRÉA & 19, R. VAVIN, PARIS”.

LF-O-CB The tube appears to have been used as it is wrinkled as if squeezed and is even covered in spots of other paint colors – red, yellow, and purple – and a few black streaks beginning from the label running down the tube. There is degradation or dirt covering the label and with a large brown spot on one side. This appears to also be along the seam of the tube at the bottom. Under the black twist cap is some blue paint. The label is brown-yellow and has the same format and S.A.R.L. value LF-PGD16.

LF-O-MB The tube appears brand new, in almost perfect condition and unused. The tube itself is lustrous and appears smooth with very minimal degradation. The only appearance of aging is a few black streaks running down from the label. Along the seam, at the bottom of the tube, there is some blue staining. The label is slightly yellowed in some parts and has the same format and typeface as LF-PGD16.

LF-O-UB The tube is much like LF-O-MB: appears brand new, in almost perfect condition, unused. It is lustrous and appears smooth with very minimal degradation, with a few black streaks running down from the label, and along the seam at the bottom of the tube, there is some blue staining. The label is white and has the same format and S.A.R.L. value LF-PGD16.

S3.2 Lefranc & Bourgeois tube

Lefranc & Bourgeois paints had also been used by many painters, including Pablo Picasso [17] and collections of the early 20th century have been studied in the literature [18]. The company was founded in 1720 by Charles La Clef, an apothecary who began to produce paint pigments for an artist who lived above his shop, situated at the crossing of rue Princesse and rue du Four in the sixth district of Paris. The 300-year-old establishment has been passed down through generations of the Lefranc family. In the 1950s, the Lefranc establishment met with the Bourgeois establishments and continues manufacturing paints from its location in Le Mans, France where it has resided since 1965, and continuing to produce a wide variety of paint materials [19].

We detail below the condition of the tube:

LB-O-FW The paint tube is a white tube with a pale-yellow twist cap. No appearance of severe degradation on the tube is observed, and the tube appears full. The paint designation written as “Blanc d’Argent Carbonate de Plomb / Flake White Basic Carbonate of Lead”, and the series is “couleurs fines à l’huile pour le tableau / fine oil colors”. Below this, the logo is a black circle with “LB” in white, with, in small text, “Marque déposée” (English translation: registered trademark) on the left and “Made in France” on the right. Below the logo is written with “lefranc & bourgeois”, with, in small text, “Le Mans” on the left and “France” on the right. Warning notices are written below this to the bottom of the tube in Italian, Spanish, Dutch and Danish.

S3.3 Valor cans

Valor paint cans were fabricated under the Établissements Expert-Bezançon, founded in 1845 [20]. This was known as one of the most famous manufacturers of ceruse in the early 20th century, with locations in Aubervilliers, close to Paris and the suburbs of Lille (Saint-André-lez-Lille), the leading location for the production of ceruse in France [21]. It was owned by Charles Expert-Bezançon, a controversial figure of the production of lead white, as he delayed the restrictive legislation to the banning of poisonous lead white at the beginning of the 20th century [22]. Historical documentation dating May 19, 1930, granted authorization of Expert-Bezançon to continue manufacturing lead white despite deep controversies with the safety and health of his workers [21]. We found archival information primarily on this dispute in the early 20th century but none for the postwar period.

We detail below the condition of each of the cans:

V-O-BC The paint can appears to have been used by Hantaï, as paint drips are seen down its side. The brand name is printed at the top with “peinture à l’huile de lin polymérisée” (English translation: paint by polymerized linseed oil, a.k.a. stand oil) printed below. The center of the can shows a simplified graphic version of the brand’s original logo, the dancing painter, in white, where a paint brush is painting a swirl around a dancing figure. The paint designation is marked by “34 Bois Clair”. Translated as ”Light wood”, we emphasize the perhaps less usual color of this can compared to the others. On the side of the can, we have a glimpse of “NORD)” printed on the back. Other photodocumentation of a Valor paint can, not used in this study, shows “…Lille (Nord)”, thus it was deduced, with literature searches, that the Valor paints were fabricated by the Expert-Bezançon establishments in one of their two locations — Aubervilliers (Seine) or Saint-André-lez-Lille (Nord) — since both are indicated on the label.

V-O-JJ There is no photodocumentation of this can.

Figure S3.1: Paint tubes and cans from Hantaï’s atelier in Paris

Table S3.2: Sample set studied in this work. CS: cross-section, GJ: 2015 sample in glass jar, PF: 2015 sample in plastic film.

Designation	**Sample name**	**Sample description**	**Analysis performed**
Lefebvre-Foinet paint tubes			
Rouge de Cadmium Cadmium Red	LF-O-CdR	GJ	C14, FT-IR, XRD, Py-GC-MS, GC-MS, HPLC
	LF-O-CdR-CS	CS of LF-O-CdR	SEM-EDX
Rouge de Cadmium Orange Cadmium Red Orange	LF-O-CdRO	PF	C14, FT-IR, XRD, Py-GC-MS, GC-MS, HPLC
	LF-O-CdRO-CS	CS of LF-O-CdRO	SEM-EDX
Rouge de Cadmium Pourpre Cadmium Red Purple	LF-O-CdRP	PF	C14, FT-IR, XRD, Py-GC-MS, GC-MS, HPLC
	LF-O-CdRP-CS	CS of LF-O-CdRP	SEM-EDX
Rouge de Cadmium Vermillon Cadmium Red Vermilion	LF-O-CdRV	GJ	C14, FT-IR, XRD, Py-GC-MS, GC-MS, HPLC
	LF-O-CdRV-CS	CS of LF-O-CdRV	SEM-EDX
Jaune de Cadmium Orange Cadmium Yellow Orange	LF-O-CdYO	PF	C14, FT-IR, XRD, Py-GC-MS, GC-MS, HPLC
	LF-O-CdYO-CS	CS of LF-O-CdRV	SEM-EDX
Jaune de Cadmium Moyen Cadmium Yellow Medium	LF-O-CdYM	PF	C14, FT-IR, XRD, Py-GC-MS, GC-MS, HPLC
	LF-O-CdYM-CS	CS of LF-O-CdYM	SEM-EDX
Vert Permanent Foncé Permanent Green Deep	LF-O-PGD4	PF	C14, FT-IR, XRD, Py-GC-MS, GC-MS, HPLC
	LF-O-PGD4-CS	CS of LF-O-PGD4	SEM-EDX
Vert Permanent Foncé Permanent Green Deep	LF-O-PGD16	GJ	C14, FT-IR, XRD, Py-GC-MS, GC-MS, HPLC
	LF-O-PGD16-CS	CS of LF-O-PGD16	SEM-EDX
Bleu Cerulean Cœrulean Blue	LF-O-CB	PF	C14, FT-IR, XRD, Py-GC-MS, GC-MS, HPLC
	LF-O-CB-CS	CS of LF-O-CB	SEM-EDX
Bleu Monacal Monacal Blue	LF-O-MB	GJ	C14, FT-IR, XRD, Py-GC-MS, GC-MS, HPLC
	LF-O-MB-CS	CS of LF-O-MB	SEM-EDX
Bleu Outremer Ultramarine Blue	LF-O-UB	GJ	C14, FT-IR, XRD, Py-GC-MS, GC-MS, HPLC
	LF-O-UB-CS	CS of LF-O-MB	SEM-EDX

Continued on next page

Table S3.2: Sample set studied in this work. CS: cross-section, GJ: 2015 sample in glass jar, PF: 2015 sample in plastic film. (Continued)

Designation	Sample name	Sample description	Analysis performed
Lefranc & Bourgeois paint tube			
Blanc d'Argent Flake White	LB-O-FW	GJ	C14, FT-IR, XRD, Py-GC-MS, GC-MS, HPLC
	LB-O-FW-CS	CS of LB-O-FW	SEM-EDX
Valor paint cans			
Bois Clair	V-O-BC	GJ	C14, FT-IR, XRD, Py-GC-MS, GC-MS, HPLC
	V-O-BC-CS	CS of V-O-BC	SEM-EDX
Jaune de Jonquille	V-O-JJ	GJ	C14, FT-IR, XRD, Py-GC-MS, GC-MS, HPLC
	V-O-JJ-CS	CS of V-O-JJ	SEM-EDX

S4 Supplementary methods

S4.1 Carbon-14 dating

Except for the LB-O-FW paint, all the samples of paint were chemically pretreated by an acid leach (HCl 0.5M) to remove fossil carbonates such as calcite and then rinsed with ultrapure water to neutral pH. In this way, the only carbon-based compounds remaining in the pretreated sample come from those deriving from the organic fraction [23]. Carbon dioxide was then produced by combustion in an Elemental Analyzer (Flash 2000, ThermoFisher Scientific) at 1800°C under oxygen flow. The CO_2 produced was separated from the other combustion gases in the analyzer and collected cryogenically [24]. Due to the presence of lead white, sample LB-O-FW was handled separately. Lead white was thermally removed [25, 26] and carbon dioxide from the organic fraction residue was obtained by combustion at 850°C with copper oxide and silver wire [24]. For all the samples, the resulting CO_2 was reduced to graphite by hydrogen over an iron catalyst. The graphite was then pressed into targets and measured with the AMS LMC14/ARTEMIS facility [27, 28]. Measurements were normalized to the OxII oxalic acid standard and corrected for background and fractionation with δ13C as measured by the AMS to determine sample activity, which are reported in units of percent modern carbon (pMC). The ^{14}C contents in pMC were converted into calendar years with the OxCal calibration program [29], using the Bomb21 NH1 post-bomb atmospheric curve [30].

S4.2 Gas chromatography – mass spectrometry (GC-MS)

GC-MS was performed at University of Pisa. GC-MS procedure for the determination of free aliphatic and terpenoid acids and free metal soaps of aliphatic and terpenoid acids. Samples (350–550 µg) were subject to an analytical procedure which consisted of two derivatization steps with silylating agents: the first step to silylate free aliphatic and terpenoid acids with hexamethyldisilizane (HMDS) at 60°C for 30 min, the second to silylate both free aliphatic and terpenoid acids and free metal soaps of aliphatic and terpenoid acids with N,O-Bis(trimethylsilyl)trifluoroacetamide (BSTFA) at 80°C for 80 min. GC-MS instrumentation consisted of an Agilent Technologies 6890N gas chromatograph coupled with a 5973 Mass Selective Detector single-quadrupole mass spectrometer. Samples were injected in splitless mode at 280°C. GC separation was performed on a fused silica capillary column HP-5MS (J&W Scientific, Agilent Technologies, stationary phase 5% diphenyl–95% dimethyl-polysiloxane, 30 m length, 0.25 mm i.d., 0.25 µm film thickness). The details of the analytical methodology and instrumental conditions are reported in La Nasa et al. [31]. Quantitation was carried out based on calibration curves for lauric, myristic, palmitic, oleic, stearic, suberic, sebacic and azelaic acids. Blank analyses were carried out to determine LOQ and LOD values

S4.3 Pyrolysis – gas chromatography – mass spectrometry (Py-GC-MS)

Py-GC-MS was performed at University of Pisa. Samples (200–300 µg) were placed into a clean stainless cup, admixed with 2 µL of HMDS and inserted into the micro-furnace. The analyses were performed using a multi-shot pyrolyzer EGA/ PY-3030D (Frontier Lab) coupled with a 6890N gas chromatography system with a split / splitless injection port and a 5973 mass selective single quadrupole mass spectrometer (Agilent Technologies, USA). Details of the operating conditions are reported in La Nasa et al. [31].

S4.4 High pressure liquid chromatography (HPLC-ESI-Q-Tof)

(Liquid chromatography / flow injection analysis)-electrospray ionization quadrupole-time of flight tandem mass spectrometry (HPLC-ESI-Q-Tof / FIA-ESI-Q-Tof). HPLC-ESI-Q-Tof / FIA-ESI-Q-Tof were performed at University of Pisa. Analyses of the lipid materials were carried out on a 1200 Infinity HPLC coupled by a Jet Stream ESI interface with a Quadrupole-Time of Flight tandem mass spectrometer 6530 Infinity Q-ToF (Agilent Technologies). The sample extractions were performed using an Ethos One microwaves oven system (Milestone Srl, Italy). The full instrument conditions both for the FIA and HPLC analysis are reported in La Nasa et al. [32, 33].

S4.5 Fourier-transform infrared (FT-IR) spectrometry

FT-IR spectrometry was performed using the Bruker Vertex 70 spectrometer at IPANEMA, equipped with a Bruker Hyperion 3000 microscope and deuterated triglycine sulfate (DTGS) far infrared extension. A small paint sample was ground into 120 g of KBr and pressed into a pellet. A 64×64 pixel image was acquired using a focal-plane array (FPA) detector (64 scans, spectral range: 4000–860 cm^{-1}) and the average spectrum for multiple zones on the image were obtained.

S4.6 Scanning electron microscopy (SEM) and energy-dispersive X-ray (EDX) spectroscopy

SEM elemental analysis was performed at IPANEMA laboratory. The SEM is a SEM-FEG Supra 55VP from Zeiss, equipped with a field emission gun microscope, with a variable pressure scanning electron (VPSE) detector and with a silicon-drift detector (SDD) from Bruker for EDX analysis. EDX analysis was performed at 15 keV for all samples, except for the Valor samples, which were characterized at 30 keV. The Cd based samples were studied in high-pressure mode while the rest of the samples were studied under partial pressure between 70–80 Pa, with a voltage collector at 275 kV. For a sufficient intensity count, the diaphragm was set at 120 mm^2, and each mapping was scanned over 180 s. Elemental analysis was carried out on CS samples, which were prepared in Technovit 2000 LC liquid, cut with a diamond wire saw and polished with SiC paper.

S4.7 X-ray diffraction (XRD)

XRD analysis was performed by synchrotron based μ-XRD at the ID22 beamline of the ESRF (Grenoble, France). These samples were studied at an incident energy of 35 keV (λ = 0.354 Å), a beam size of $\sim 1 \times 1$ mm^2, and an energy resolution of 0.0025° (2θ, FWHM at 35 keV). The diffracted photons were measured on a cadmium telluride (CdTe) pixel detector (EIGER2 2M-W) positioned along the 2θ circle and behind a set of thirteen Si(111) analyzer crystals [34]. The diffractograms were taken in the 2θ range 0.002–44°. crystal phases were identified from the PDF-4+ database. For Cd based pigments CdS_xSe_{1-x}, the elemental ratio x of Se was estimated using the linear correlation between the diffraction spacing and content (Supplementary Text S8.2).

S5 Additional dating results

S5.1 Archival information on paint logos

Archival information on the logos was used to complement the ^{14}C dating results.

The Lefranc & Bourgeois tube could be dated based on the manufacturing location indicated on the tube. “Le Mans” was written on LB-O-FW, indicating Le Mans, France. This manufacturing site was established in 1965 [19], and thus provides the cut-off date, therefore the date was concluded to be after this date.

Another example involves the Valor paint can for sample V-O-BC. The paint can is dark green with a white logo representing the “dancing painter” (*Le peintre dansant*) (Fig. S3.1e). Édouard Boubat documented Valor cans in 1968 at Hantaï’s workshop in Meun when he was creating the *Meuns* series (Fig.S5.1a), which were also dark green with a logo similar to the one on the Valor can for sample V-O-BC. Only one side of the can for sample V-O-BC was documented. Therefore, we compared this can with another Valor can in Hantaï’s workshop with the same white modernized dancing painter. This can bears the inscription “creation by R. Gid”[1] (Fig. S5.1d). Raymond Gid was a 20th-century graphic artist, and it has been documented that he designed an advertisement for Valor paints in 1966 (Fig. S5.1d), which featured the modernized logo [35]. Hantaï’s documented use of paint cans and the use of the modernized dancing painter logo by Raymond Gid in 1966, confirms that the Valor paint can in question was unlikely to have been manufactured as late as the 1990s; therefore, we conclude that the date of the oil is 1958. A presumably older version of the logo has been documented on another paint can (Fig. S5.1b) from Hantaï’s workshop and on a calendar (Fig. S5.1c) sold by Valor in 1962, depicting the dancing painter as a young, red-haired dancer in a white dress painting a multicolor circle around themselves. At this stage of the research we ignore whether the two logos coexisted, whether there was a significant period of time between the production of the oil and its packaging, or whether the date 1958 should be further discussed. We have therefore indicated the date as “1958(?)”.

---

[1] Original text in French: ”création R. GID”

Figure S5.1: Valor documentation found in this study: Hantaï photographed by Édouard Boubat in 1968 in Meun, France, with Valor cans (a); a Valor can from Hantaï's studio exhibiting the pre-1966 dancing painter logo (b); a book dating 1962 exhibiting the pre-1966 dancing painter logo (c); a Valor can from Hantaï's studio exhibiting the post-1966 dancing painter logo, citing R. Gid as the creator (d); and an advertising poster from 1966 with the modernized "dancing painter" logo by Raymond Gid (e).

S5.2 Additional information on carbon-14 dating interpretation

An increase in the fraction of ^{14}C in the atmosphere appears in the 1950s due to nuclear tests, known as the “bomb peak”. This fraction increases from 1953 onwards, reaches its maximum around 1965 and slowly decreases until today. This peak is used as a calibration curve to convert ^{14}C content into dates. For contemporary materials, a single ^{14}C content thus leads to the identification of two possible date ranges, one before, the other after the bomb peak. Small fluctuations of the calibration curve cause for date ranges rather than the identification of a specific year. For example, for the case of LF-O-CdRV, the ^{14}C dating estimates the age of the linseed oil in the sample at either 1963 or 1973–1974. The range is due to a small fluctuation on the curve between 1973 and 1974, thus both years are possible options. Combining this measure with photodocumentation allowed us to determine the date.

Table S5.1: Estimated dates from the carbon-14 dating results and the estimated date determined by the label description.

Sample	C14 dating	Label description	Estimated date
LF-O-CdR	1963; 1969–1971	Only tube with this value, text on label in sans serif font, resembling tubes dated in late 1960s, early 1970s (50.000)	1969–1971
LF-O-CdRO	1962–1963; 1973-1974	Text on label in serif font, value in old francs (1.700.000)	1962–1963
LF-O-CdRP	1958–1959; 1988-1989	Text on label in serif font, value in old francs (1.700.000)	1958–1959
LF-O-CdRV	1963; 1970–1972	Text on label in serif font, value in old francs (1.700.000)	1963
LF-O-CdYO	1963; 1967–1968	Text on label in serif font, value in old francs (1.700.000)	1963
LF-O-CdYM	1962–1963; 1974–1975	No capital value but text on label in serif font, resembling tubes dated in early 1960s	1962–1963
LF-O-PGD4	1963; 1964–1965	No capital value but text on label in serif font, resembling tubes dated in early 1960s	1963–1965
LF-O-PGD16	1963; 1970–1972	Text on label in sans serif font, value in new francs (17.000)	1970–1972
LF-O-CB	1963; 1966–1967	Capital value is not legible, but text on label in sans serif font, resembling tubes dated in late 1960s, early 1970s	1966–1967
LF-O-MB	1963; 1979	Text on label in sans serif font, value in new francs (17.000)	1979
LF-O-UB	1963; 1970–1972	Text on label in sans serif font, value in new francs (17.000)	1970–1972
LB-O-FW	1958–1959; 1987–1990	“Le Mans” written on tube indicates after moving Lefranc & Bourgeois headquarters in 1965	1987–1990
V-O-BC	1958; 1991–1993	Modernized dancing painter (“peintre dansant”) logo established 1966, Hantaï’s use in 1968	1958(?)
V-O-JJ	1963; 1966–1967	No photodocumentation	1963 or 1966–1967

S6 Additional results of organic analysis

S6.1 GC-MS chromatographic profiles

The samples were analyzed by GC-MS to obtain the qualitative and quantitative profiles of free aliphatic and terpenoid acids and free metal soaps of aliphatic and terpenoid acids. With this procedure, we obtained two chromatograms for each sample: one showing the profile of free aliphatic and terpenoid acids, named FFA (HMDS), and the other showing the profile of the sum of free aliphatic and terpenoid acids, and free metal soaps of aliphatic and terpenoid acids, named FFA + FMS (BSTFA). The relative content of free aliphatic and terpenoid acids, and free metal soaps of aliphatic and terpenoid acids was determined for each sample using calibration curves. With this approach, it was possible to obtain a comparison of the qualitative and quantitative profiles of free species and metal soaps. It is important to keep in mind that, as the content of pigments and other inorganic additives was not known, only a relative quantitation may be carried out.

S6.1.1 Quantitative GC-MS data

Table S6.1: Ratios from the mass spectrometry analysis. A/P: azelaic/palmitic, P/S: palmitic/stearic, O/S: oleic/stearic, M/S: myristic/stearic.

Sample name	**Fraction**	**A/P**	**P/S**	**ΣD%**	**O/S**	**M/S**	**weight%**
Lefebvre-Foinet paint tubes							
LF-O-CdR	FFA + FMS (BSTFA)	0.1	2.7	0.1	1.2	0.1	3.1%
	FFA (HMDS)	0.0	2.8	0.0	1.3	0.0	1.7%
					FMS (BSTFA − HMDS):		1.4%
LF-O-CdRP	FFA + FMS (BSTFA)	0.7	1.8	0.3	0.9	0.1	2.4%
	FFA (HMDS)	0.1	2.0	0.1	0.9	0.0	1.2%
					FMS (BSTFA − HMDS):		1.2%
LF-O-CdRV	FFA + FMS (BSTFA)	0.1	2.9	0.1	1.0	0.1	3.3%
	FFA (HMDS)	0.0	3.3	0.0	0.8	0.0	1.9%
					FMS (BSTFA − HMDS):		1.4%
LF-O-CdYO	FFA + FMS (BSTFA)	0.5	2.8	0.3	1.2	0.1	7.6%
	FFA (HMDS)	0.4	2.8	0.2	1.2	0.1	5.4%
					FMS (BSTFA − HMDS):		2.2%
LF-O-CdYM	FFA + FMS (BSTFA)	0.2	2.5	0.1	1.3	0.2	6.0%
	FFA (HMDS)	0.1	3.1	0.1	1.5	0.0	4.3%
					FMS (BSTFA − HMDS):		1.7%

Continued on next page

Table S6.1: Ratios from the mass spectrometry analysis. A/P: azelaic/palmitic, P/S: palmitic/stearic, O/S: oleic/stearic, M/S: myristic/stearic. (Continued)

Sample name	**Fraction**	**A/P**	**P/S**	**ΣD%**	**O/S**	**M/S**	**weight%**
LF-O-PGD-4	FFA + FMS (BSTFA)	0.4	3.2	0.2	1.2	0.0	5.7%
	FFA (HMDS)	0.1	3.3	0.0	1.3	0.0	3.2%
					FMS (BSTFA − HMDS):		2.5%
LF-O-PGD-16	FFA + FMS (BSTFA)	2.6	2.3	0.7	0.5	0.1	5.8%
	FFA (HMDS)	1.5	2.2	0.5	0.4	0.1	2.0%
					FMS (BSTFA − HMDS):		3.8%
LF-O-CB	FFA + FMS (BSTFA)	1.1	2.4	0.5	0.1	0.0	8.4%
	FFA (HMDS)	1.0	2.5	0.5	0.0	0.0	6.3%
					FMS (BSTFA − HMDS):		2.2%
LF-O-MB	FFA + FMS (BSTFA)	0.3	3.2	0.2	1.6	0.1	6.8%
	FFA (HMDS)	0.1	3.4	0.1	1.7	0.0	4.9%
					FMS (BSTFA − HMDS):		1.9%
LF-O-UB	FFA + FMS (BSTFA)	0.5	2.7	0.3	0.8	0.1	6.4%
	FFA (HMDS)	0.2	3.0	0.1	0.9	0.1	5.8%
					FMS (BSTFA − HMDS):		1.8%
Lefranc & Bourgeois paint tube							
LB-O-FW	FFA + FMS (BSTFA)	0.2	1.6	0.1	0.7	0.1	7.6%
	FFA (HMDS)	0.0	0.8	0.0	1.0	0.0	0.5%
					FMS (BSTFA − HMDS):		7.1%
Valor paint cans							
V-O-BC	FFA + FMS (BSTFA)	0.9	1.4	0.3	1.4	0.2	2.2%
	FFA (HMDS)	1.1	1.4	0.3	1.8	0.1	1.6%
					FMS (BSTFA − HMDS):		0.6%
V-O-JJ	FFA + FMS (BSTFA)	0.3	1.7	0.1	2.1	0.0	7.8%
	FFA (HMDS)	0.0	1.7	0.0	2.3	0.0	5.4%
					FMS (BSTFA − HMDS):		2.4%

S6.1.2 Addition of free fatty acids

The GC-MS chromatograms did not show any unusual profile of saturated fatty acids (lauric and myristic acids were always detected but never particularly high — see M/S ratio in Table S6.1), and they always featured the presence of dicarboxylic and unsaturated acids. The data highlight the natural hydrolysis of the oil binder and did not show any evidence of the addition of free fatty acids to the paint formulation, preventing us to draw any definitive conclusions on this aspect.

S6.1.3 Stage of curing

The pigment composition has an effect on the curing of the paint, which was observed by variable stages of curing and oxidation between samples. This observation is based on the relative content of azelaic acid (Tab. S6.1) and the molecular pattern of unsaturated fatty acids (Fig. S6.1). For example, the paint based on Co blue (LF-O-CB) had the most advanced stage of curing, which is an expected result as Co(II) salts are oxidative driers [36, 37]. On the other hand, the Cd based paints presented, in general, a less advanced stage of curing, in agreement with the slow drying nature of Cd based pigments [38]. Different curing state can also be a result of Lefebvre-Foinet's paint making process, reported to expose their oils to sunlight for long periods of time in order to offer different oil properties, having an impact on the color, rheological properties and drying time of the binder [39].

S6.1.4 *Pinaceae* resin

The detection of 7-oxo-dehydroabietic acid and dehydroabietic acid in the GC-MS chromatograms of the Valor paints indicated the use of a resin extracted from a conifer tree of the *Pinaceae* (pine) family. Interestingly, a mixture of a drying oil and a conifer resin was also found in the paints of the renewed Ripolin brand, produced in the Netherlands. Gloss, durability and good handling properties made enamel paints highly appreciated by artists, especially until the 1940's. These usually contained hard fossil resins, such as copal, and were added with small amounts of rosin or colophony (from the *Pinaceae* family), to prevent the charring of fossil resins [40]. Fossil resins were not detected in any of the samples analyzed. Oleoresinous enamel paints required prolonged heating in different stages of their production. The aim was to pre-polymerize the oil, to give it body and to shorten its drying time [18].

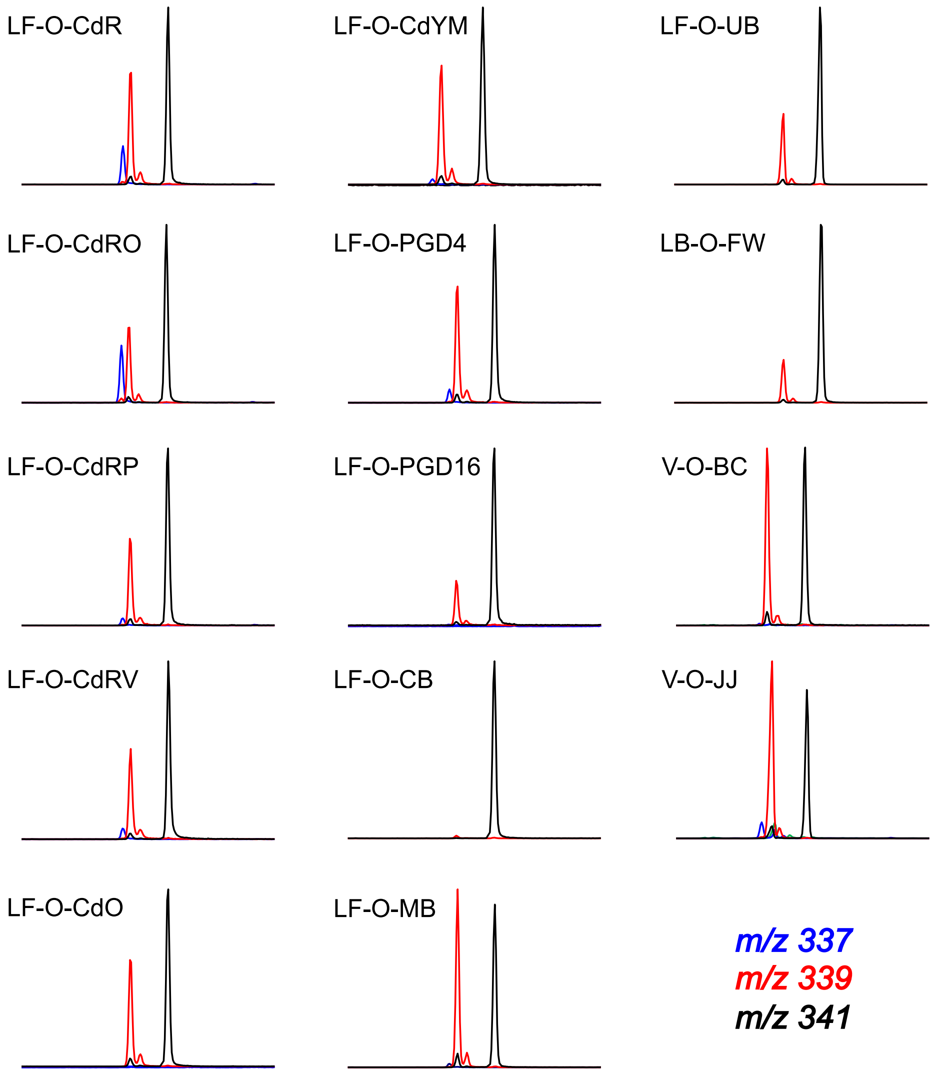

Figure S6.1: GC-MS chromatographic profiles of linoleic acid (TMS ester; m/z 337, blue); oleic acid (TMS ester; m/z 339, red); stearic acid (TMS ester; m/z 341, black) from the chromatograms relative to free fatty and dicarboxylic acids and free metal soaps of fatty and dicarboxylic acids

S6.2 HPLC interpretation

The analysis highlighted palmitic, linoleic oleic, and stearic acids as main unoxidized free fatty acids, while mono- and di-hydroyl derivatives of oleic, linoleic and linolenic acids were detected as main oxidized species. The glyceride fraction comprised species with the following substituents: A: arachidyl ($C_{20:0}$), B: behenyl ($C_{22:0}$), L: linoleyl ($C_{18:2}$), O: oleyl ($C_{18:1}$), S: stearyl ($C_{18:0}$), P: palmityl ($C_{16:0}$), and $C_{n:m,i\mathrm{OH}}$: linear aliphatic acyl substituent with n carbon atoms, m unsaturations, and i hydroxyl moieties. The MAG fraction was characterized by the presence of mono-palmitin (m/z 353.3, [M+Na]$^+$), mono-olein (m/z 379.3, [M+Na]$^+$), and mono-stearin (m/z 381.3, [M+Na]$^+$). The DAGs were characterized by the presence of PP (m/z 591.5, [M+Na]$^+$), PO (m/z 617.5, [M+Na]$^+$), PS (m/z 619.5, [M+Na]$^+$), and SS (m/z 647.5, [M+Na]$^+$). Among the oxidized DAGs, the most abundant were the m/z 663.5 ($C_{18,\mathrm{OH}}$S, [M+Na]$^+$), m/z 661.5 ($C_{18:1,\mathrm{OH}}$S, [M+Na]$^+$), and m/z 695.5 ($C_{18:2,\mathrm{OH}}$S, [M+Na]$^+$). The triacylglycerols (TAG) fractions were mainly characterized by the presence of LLP (m/z 877.7, [M+Na]$^+$), PLP (m/z 853.7, [M+Na]$^+$), LOP (m/z 879.7, [M+Na]$^+$), OOL (m/z 905.7, [M+Na]$^+$), POP (m/z 855.7, [M+Na]$^+$), OOP (m/z 881.7, [M+Na]$^+$), OOO (m/z 907.8, [M+Na]$^+$), OSP (m/z 883.8, [M+Na]$^+$), OOS (m/z 909.8, [M+Na]$^+$), and OSS (m/z 911.8, [M+Na]$^+$). The oxidized portion of TAGs was mainly characterized by the presence of species deriving from the oxidation of TAGs containing polyunsaturated fatty acids as acyl substituents (linoleic and linolenic acids). In detail isomers of m/z 895.7 ($C_{18:2,\mathrm{OH}}$OP, [M+Na]$^+$), 897.7 ($C_{18:1,\mathrm{OH}}$OP, [M+Na]$^+$), 899.7 ($C_{18,\mathrm{OH}}$OP, [M+Na]$^+$), 911.7 ($C_{18:2,\mathrm{OH}}C_{18:1,\mathrm{OH}}$P, [M+Na]$^+$), 927,7 ($C_{18:1,2\mathrm{OH}}C_{18:2,\mathrm{OH}}$P, [M+Na]$^+$), 937.7 ($C_{18:2,\mathrm{OH}}C_{18:2,\mathrm{OH}}$S, [M+Na]$^+$), and 955.7 ($C_{18:1,2\mathrm{OH}}C_{18:1,\mathrm{OH}}$O, [M+Na]$^+$) were detected. These chromatographic profiles can be ascribed to linseed oil. Only two samples, LF-O-CdRP and LF-O-PGD16, contained triacylglycerol with long chain acyl substituents, including ALL (m/z 833.8, [M+Na]$^+$), ALO (m/z 935.8, [M+Na]$^+$), ALS (m/z 937.8, [M+Na]$^+$), and BLO (m/z 963.8, [M+Na]$^+$), which can be associated to the presence of safflower oil.

S6.2.1 Type of oil

As described in the main text, linseed oil was the oil identified in all the samples analyzed. Safflower (*Carthamus tinctorius* L.) oil was additionally detected in samples LF-O-CdRP, dated in 1958, and LF-O-PGD16 dated in 1972. The two paint tubes were produced in two different periods, more than ten years apart, thus the occurrence of safflower oil cannot be related to the same batch of an oil blend. Safflower oil is a semi-drying oil, and is thus a slow drying oil. Its combination with Cd red, which slows down the oil curing, seems unusual. Interestingly, LF-O-PGD16 contains traces of cobalt, probably added as a paint dryer. Safflower oil has the tendency to favor oxidative degradation over cross-linking, and indeed both LF-O-CdRP and LF-O-PGD16 present a relatively high degree of oxidation, in comparison, respectively, to the other Cd and Cr containing paints (Tab. S6.1). Safflower oil has a reduced tendency to yellowing compared to linseed oil, making it a precious ingredient of white, blue and pale colored oil paints. The presence of safflower oil in Lefebvre-Foinet has been cited by artists who purchased products from Lefebvre-Foinet, but mainly for white pigments in preparation layers of canvases [16, 39]. The addition of safflower oil to these specific pigments is not entirely understood, as it does not appear to be related to any specific period or pigment.

S6.2.2 Beeswax

The lipid profiles of samples LF-O-CdRP and LF-O-UB presented high molecular weight esters, which suggested the presence of beeswax. To confirm this, these samples were subject to FIA-MS analysis (Fig. 5 in the main manuscript), which showed three different ion clusters. Besides the ions associated to the presence of an oxidized drying oil, m/z associated to monoesters, diesters, and triesters of long chain alcohols and fatty acids are detected. In particular, the mass spectral pattern may be ascribed to esters of palmitic and 15-hydroxyhexadecanoic acids with long chain alcohols, which can be unambiguously ascribed to beeswax [32].

S6.3 FT-IR spectroscopy analysis

FT-IR analysis was performed to facilitate the identification of both organic and inorganic materials present in the paints, with a particular emphasis on the characterization of the binding media and potential degradation products. The interpretation of the FT-IR spectra confirmed that oil was present as binding medium in all the paints, as evidenced by its characteristic absorption bands, including the stretching vibrations of CH_2 appearing at 2925 and 2855 cm^{-1}, the C=O (ester) stretching band at approximately 1740 cm^{-1}, the C−H bending bands at 1460 and 1381 cm^{-1}, and the C−O stretching bands at 1238, 1164 and 1100 cm^{-1} [41, 42, 43]. Furthermore, the absence of the olefinic C−H stretching band at 3010 cm^{-1} [44], the broad O−H stretching band centered at 3440 cm^{-1} [41] and the waveform of the band at 1740 cm^{-1} [42] confirmed that the oil had undergone curing reactions. The appearance of a weak absorption at 1630 cm^{-1} related to the formation of conjugated double bonds [42, 45] was observed in LB-O-FW, LF-O-CB, LF-O-CdYO, LF-O-CdR, LF-O-CdRV and LF-O-CdYM. Isomerization of double bonds with formation of conjugated systems is common in the curing of oil paints [46], and Co based dryers are known to favor this phenomenon [36, 37]. LF-O-CB also displayed a marked shift from 1630 cm^{-1} to 1640 cm^{-1}, which could be attributed to the presence of oxalates, as indicated by the accompanying absorption band at 1320 cm^{-1} [47]. The formation of oxalates was observed in LF-O-CdR and LF-O-CdRO, as well. The pigment was identified in few samples, when the chromophore is active in the mid-infrared range. For example, the Si−O stretching bands (1036 and 1013 cm^{-1}) in LF-O-UB are compatible with the presence of ultramarine blue [48] as suggested by the name of the tube, while the presence of the Cr based pigment in LF-O-PGD4 and 16 could be confirmed by the bands at 953 and 883 cm^{-1} ascribable to the symmetric and antisymmetric stretching of CrO_3 in the chromate group anion [49, 50] (Fig. S6.3a,b). In addition, the characteristic stretching bands of OH and CO_3^{2-} of lead white were identified in sample LB-O-FW at 3534 and 1045 cm^{-1}, respectively [44].

In most of the analyzed samples, a bridge-like broadband in the carboxylate region was observed, which posed challenges for the unambiguous attribution of individual peaks to specific carboxylate species. However, by leveraging complementary investigations, such as SEM-EDX and XRD, it was possible to achieve a more comprehensive understanding of the sample's chemical composition and to make reasonable inferences regarding the identity and origin of the observed carboxylates features. The presence of Cd together with the presence of the diagnostic band at $\sim$1544 cm^{-1} in the FT-IR spectra, suggested the presence of Cd carboxylates, possibly in a crystal form [51]. Other additional peaks appeared inconspicuously as a broad band, suggesting the presence of various amorphous carboxylate species. Notably, sample LF-O-CdRO, LF-O-CdRP and LF-O-CdRV showed clearly peaks at approximately 1544, 1595 and 1535 cm^{-1} (Fig. S6.2b1,c1,d1). The first peak was consistent with the bands of Cd-carboxylates [51], while the last two with amorphous and crystal Zn carboxylates respectively (Fig. 6 in the main manuscript). SEM analysis detected Zn in trace amounts of the red pigments, which could be due to the addition of Zn stearates commonly added as pigment extenders [52]. It is worth mentioning that in the sample LF-O-CdYM, a clear peak was detected at 1570 cm^{-1} (Fig. S6.2f1) along with several weak shoulders in the carboxylate region, suggesting the possible presence of carboxylate compounds in the sample. However, the peak did not match the characteristic one of Cd carboxylates, leaving the specific attribution uncertain. Similar trends were observed in samples LF-O-PGD4 and LF-O-MB, which contained evident but uncertain peaks in the carboxylate region at 1546 and 1507 cm^{-1} (Fig. S6.3a1,d1), respectively. This may lead to the hypothesis that in these samples, as well as in those where Pb and Zn do not belong to the pigment phase, metal soaps were not formed exclusively through the interaction of the pigment and the binder, but intentionally added to the paints as dispersion agents [52]. However, the low concentration of added metal soaps limited the detection and the assignments.

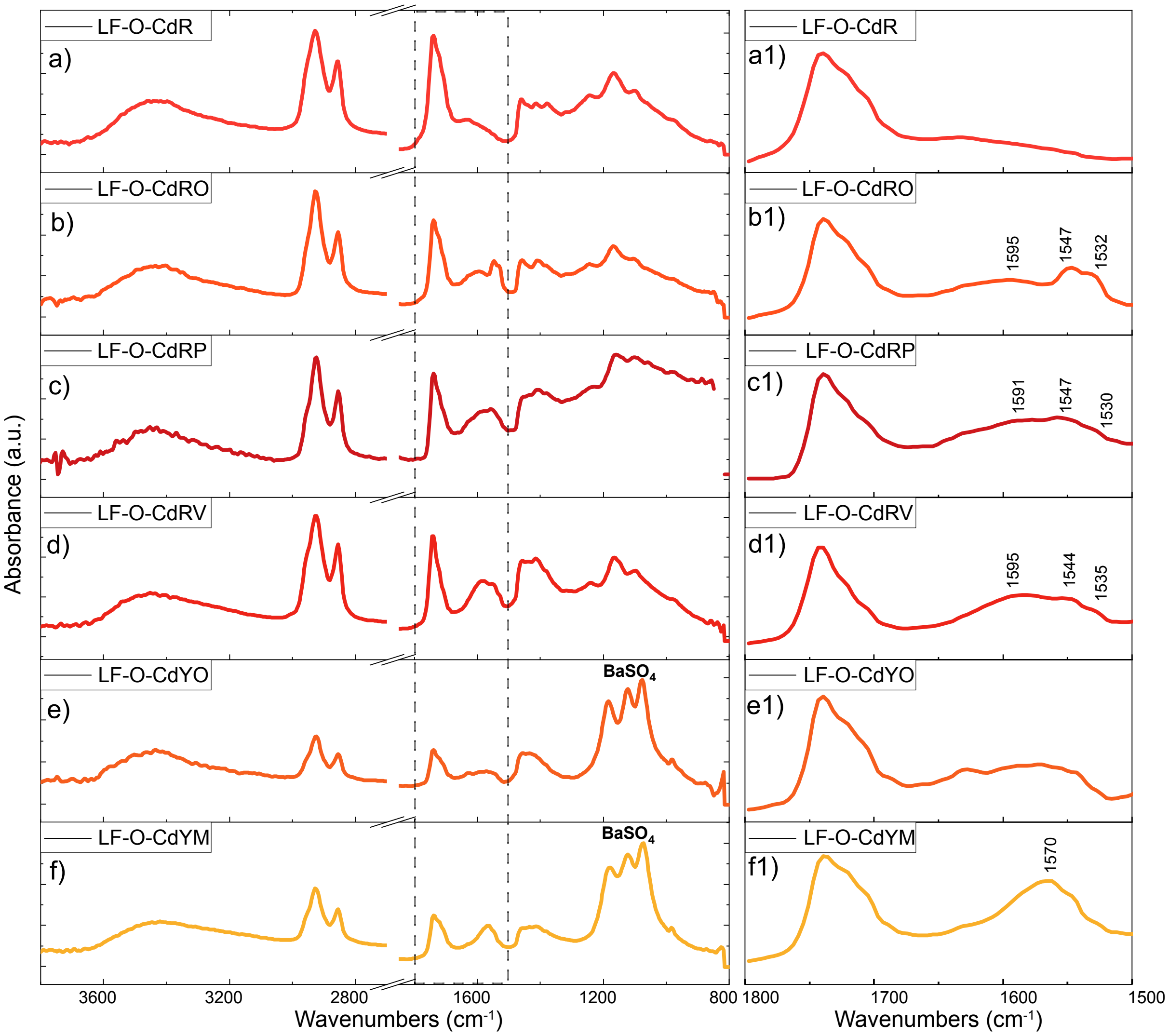

Figure S6.2: Spectra of Cd based pigments; (a–f) full spectra of the pigments; (a1–f1) ordinate expanded region of double bonds.

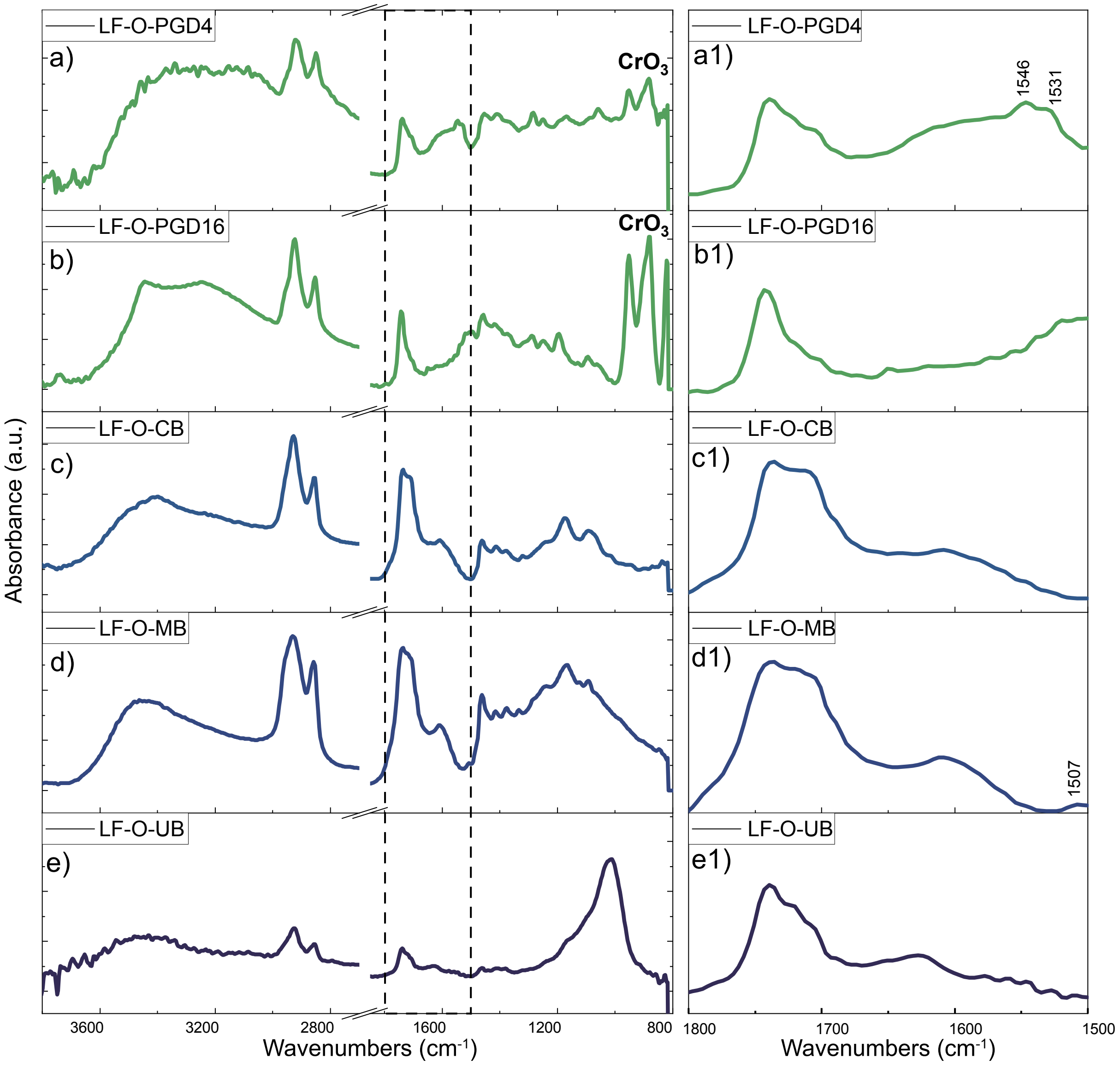

Figure S6.3: Spectra of green and blue pigments LF-O-PGD4, LF-O-PGD-16, LF-O-CB, LF-O-MB and LF-0-UB; (a–e) full spectra of the pigments; (a1–e1) ordinate expanded region of double bonds.

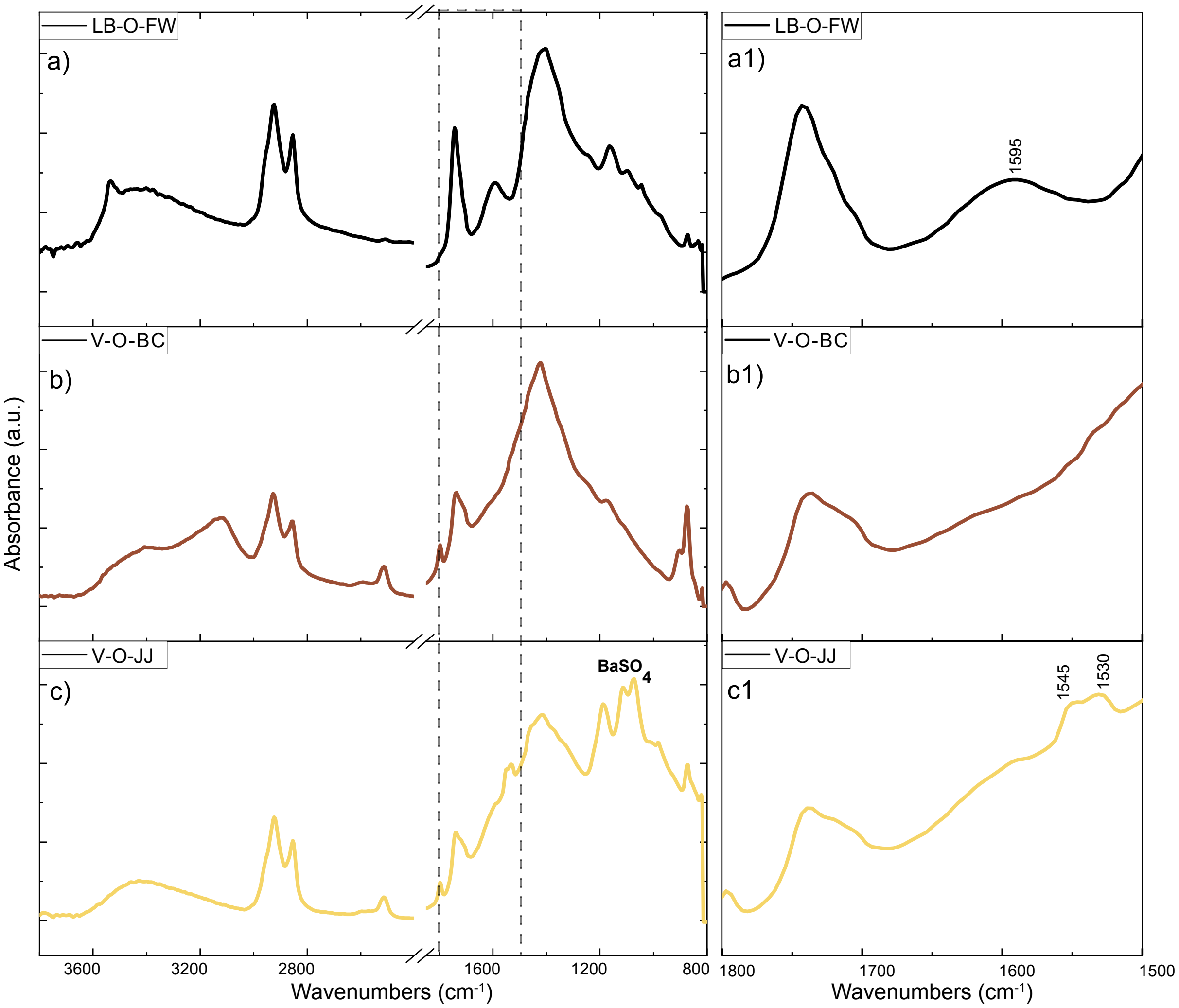

Figure S6.4: Spectra of pigments LB-O-FW, V-O-BC and V-O-JJ; (a–c) full spectra of the pigments; (a1–c1) ordinate expanded region of double bonds.

S7 Additional results from light microscopy and SEM-EDX analysis

SEM-EDX analysis was performed to identify the elemental composition and characterize the distribution of compounds in paint cross-sections. In general, higher concentration of elements related to the pigment was found in the cross-section in zones attributed to the bulk material. Higher concentration of organics (carbon, oxygen) was found in zones attributed to the dried paint. This result was hypothesized as a possible effect of phase separation between the apolar components of the oil binder and polar components of the forming metal soap, or an effect of sedimentation in the sample. The presence of Al-containing agglomerates was detected in the samples by SEM in several Cd-based paints (LF-O-CdR, LF-O-CdRO, LF-O-CdRP, LF-O-CdYO, and LF-O-CdYM), lead white (LB-O-FW) and Zn yellow (V-O-JJ). SEM mapping identified $\sim 10\,\mu m$ diameter Al oxide particles, presumably Al_2O_3, while the phase could not be confirmed by XRD. Alumina could potentially provide a substrate for organic dyes (lake pigments), which were not further investigated in this study. Si was also found in trace amounts of the pigment and, notably, $\sim 20\,\mu m$ diameter SiO_2 sized grains in two Cd based paints (LF-O-CdRO and LF-O-CdYM). Al and Si are mostly concentrated in zones where elements related to the pigment — Cd, S and Se — are localized. Minor trace elements include Zn, P, and Ba, and are also localized where there is a high concentration of pigment elements. The dark grains in the SEM images correspond to C, identified as an impurity from metallizing the CS for EDS analysis under high pressure conditions.

LF-O-CdR

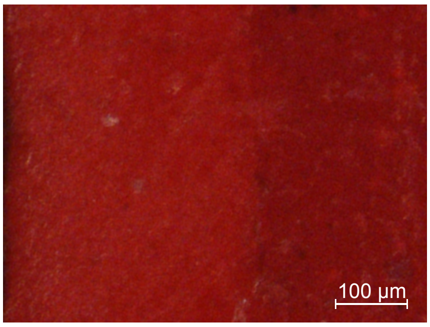

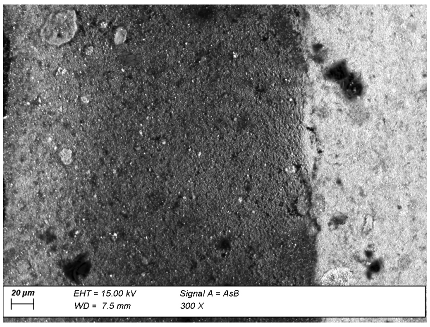

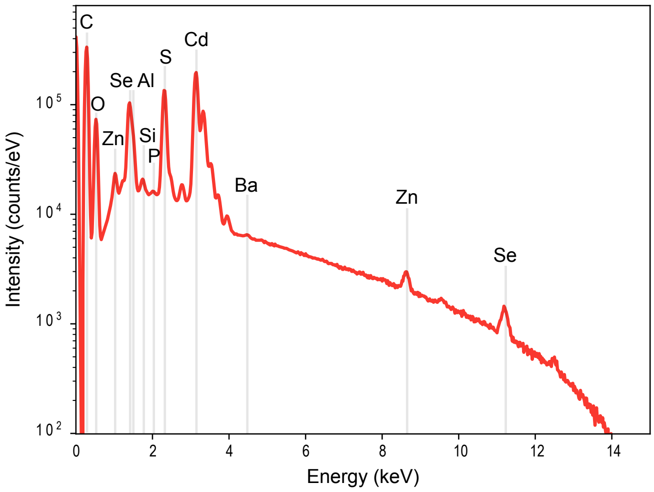

Element	A	Net	Mass. [%]	Atom.[%]
C	6	1147665	36	68
O	8	273604	13	19
Cd	48	1674932	30	6
S	16	621693	6	4
Se	34	418391	6	2
Al	13	145926	2	1
Zn	30	8273	1	0
Si	14	26186	0	0
P	15	4903	0	0
Ba	56	2084	0	0

LF-O-CdRO

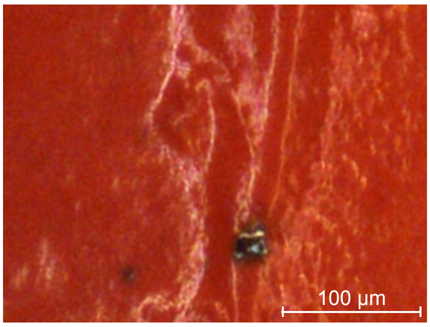

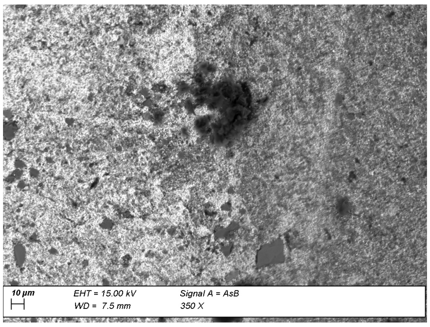

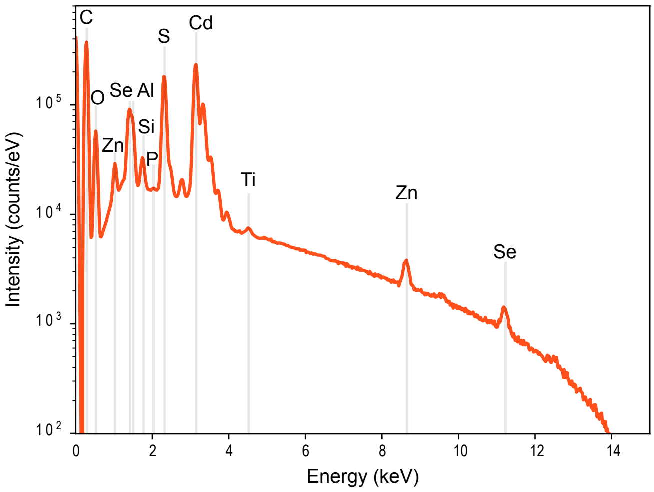

Element	A	Net	Mass. [%]	Atom. [%]
C	6	1192397	38	71
O	8	200239	10	14
Cd	48	1852267	32	6
S	16	795558	7	5
Al	13	202205	2	2
Se	34	329700	5	1
Si	14	73441	1	1
Zn	30	13729	1	0
Ti	22	6089	0	0
P	15	2357	0	0

LF-O-CdRP

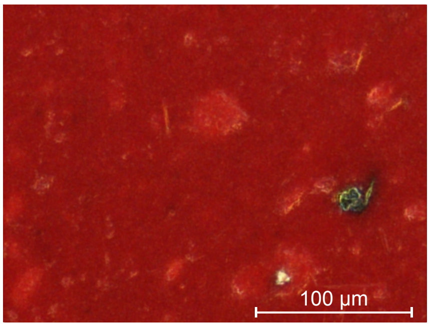

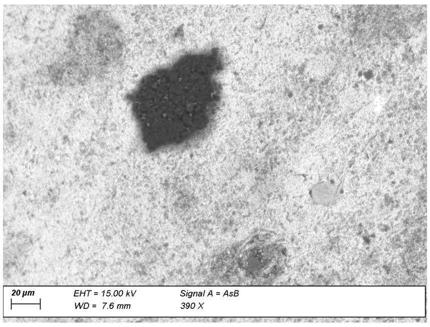

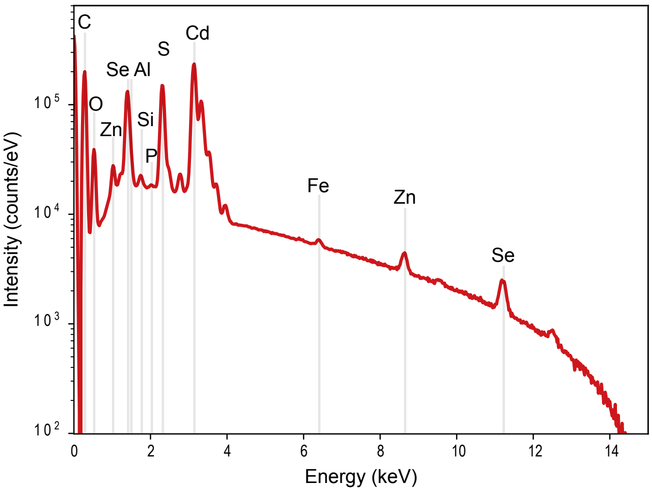

Element	A	Net	Mass. [%]	Atom. [%]
C	6	892587	27	65
O	8	162571	7	13
Cd	48	2633787	41	11
S	16	887944	7	7
Se	34	741060	9	3
Zn	30	14653	1	1
Si	14	28545	0	0
Fe	26	6601	0	0
P	15	4659	0	0

LF-O-CdRV

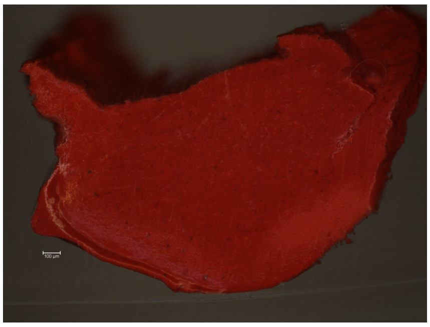

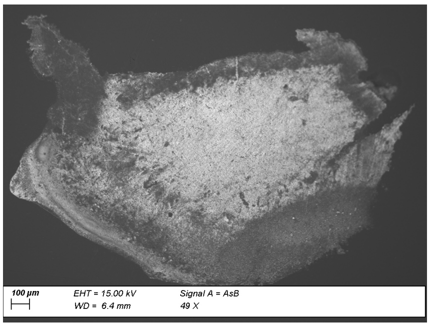

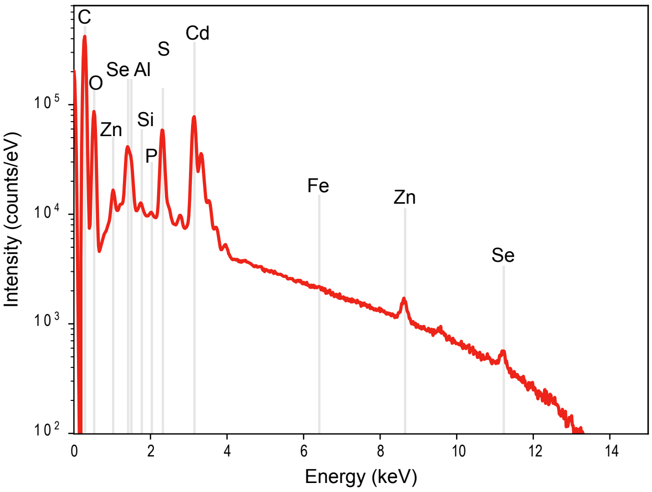

Element	A	Net	Mass. [%]	Atom. [%]
C	6	1757029	50	73
O	8	386641	20	22
Cd	48	774494	16	2
S	16	306679	3	2
Al	13	99277	1	1
Se	34	164104	2	1
Zn	30	5382	1	0
Si	14	12315	0	0
P	15	4015	0	0

LF-O-CdYO

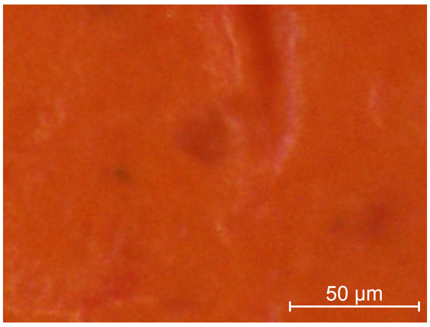

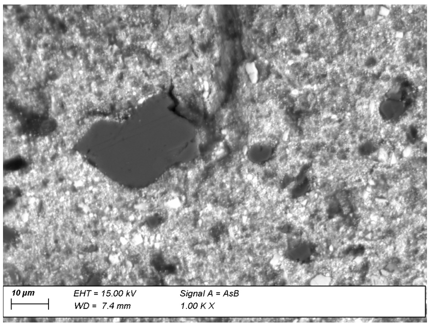

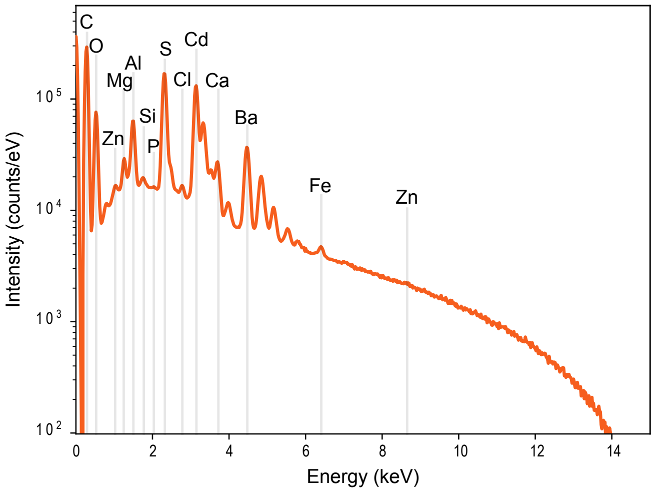

Element	A	Net	Mass. [%]	Atom. [%]
C	6	1178764	37	67
O	8	322178	14	19
S	16	945766	8	5
Cd	48	1303614	21	4
Ba	56	403024	11	2
Al	13	244981	2	2
Ca	20	109880	2	1
Mg	12	63167	1	1
Si	14	18464	0	0
Fe	26	6951	0	0
Cl	17	14680	0	0
Zn	30	596	0	0
P	15	2346	0	0

LF-O-CdYM

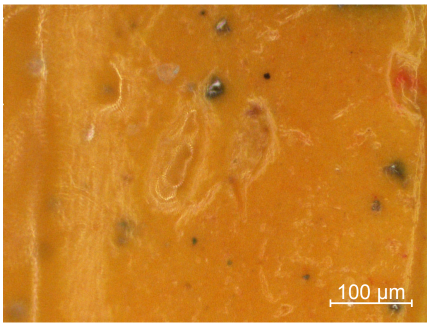

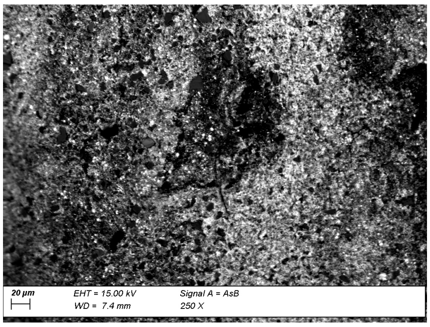

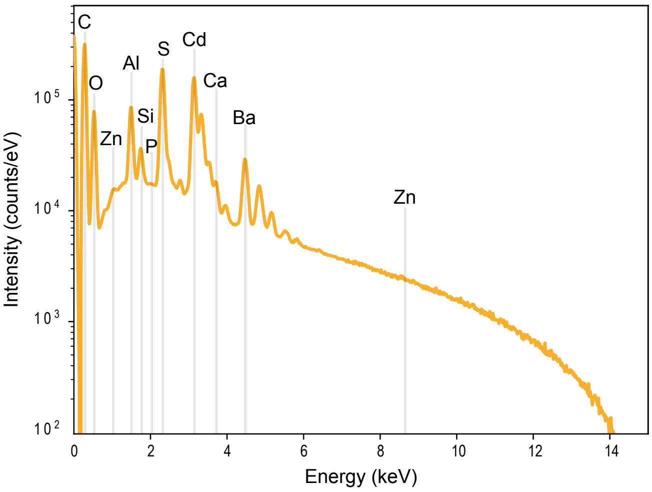

Element	A	Net	Mass. [%]	Atom. [%]
C	6	1342558	35	67
O	8	343527	13	18
S	16	1066100	7	5
Cd	48	1596763	21	4
Al	13	361210	3	3
Ba	56	296476	8	1
Si	14	107148	1	1
Ca	20	27458	0	0
Zn	30	512	0	0

LF-O-PGD4

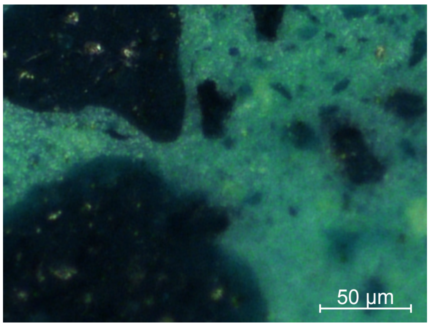

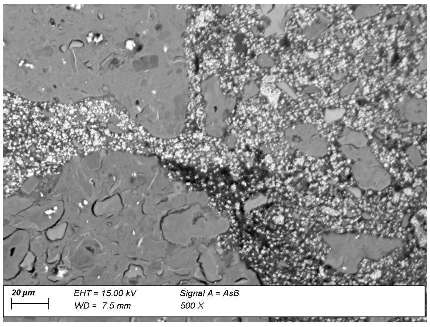

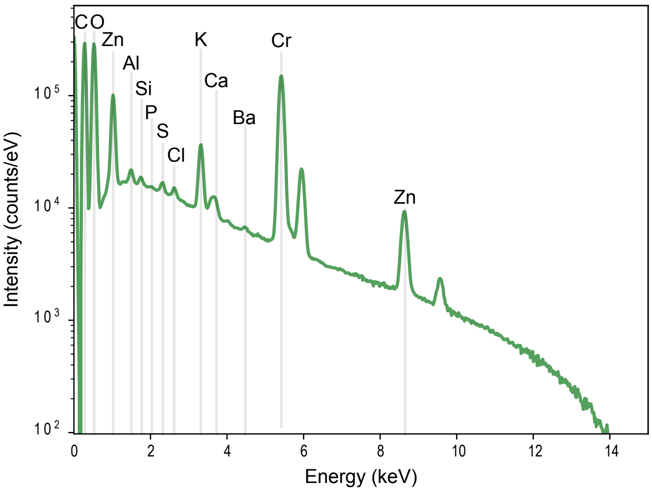

Element	A	Net	Mass. [%]	Atom. [%]
C	6	1218380	36	55
O	8	1076186	28	33
Cr	24	1218370	25	9
Zn	30	75075	6	2
K	19	195915	2	1
Ca	20	28409	0	0
Al	13	21354	0	0
S	16	20126	0	0
Cl	17	19141	0	0
Si	14	13636	0	0
Ba	56	11614	0	0
P	15	2103	0	0

LF-O-PGD16

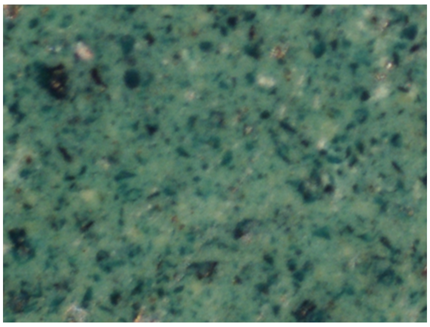

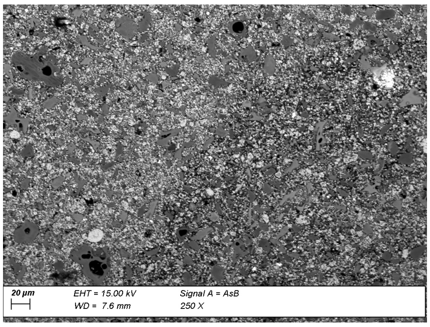

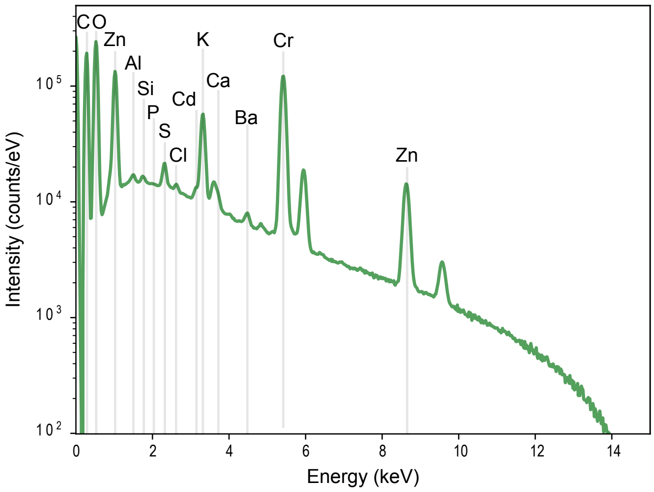

Element	A	Net	Mass. [%]	Atom. [%]
C	6	794555	26	50
O	8	951097	24	35
Cr	24	975157	18	8
Zn	30	125560	11	4
K	19	330286	3	2
S	16	49651	0	0
Ca	20	22649	0	0
Cd	48	32645	0	0
Ba	56	22813	1	0
Al	13	10212	0	0
Cl	17	11321	0	0
Si	14	8334	0	0
P	15	1194	0	0

LF-O-CB

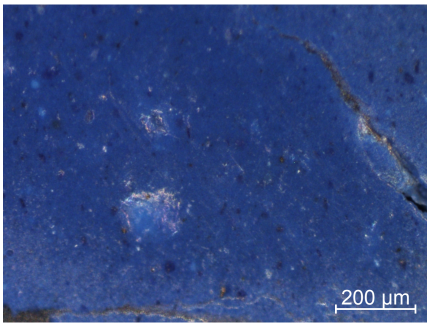

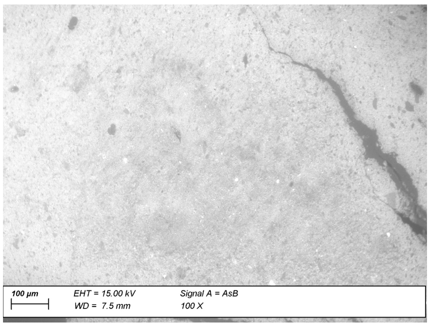

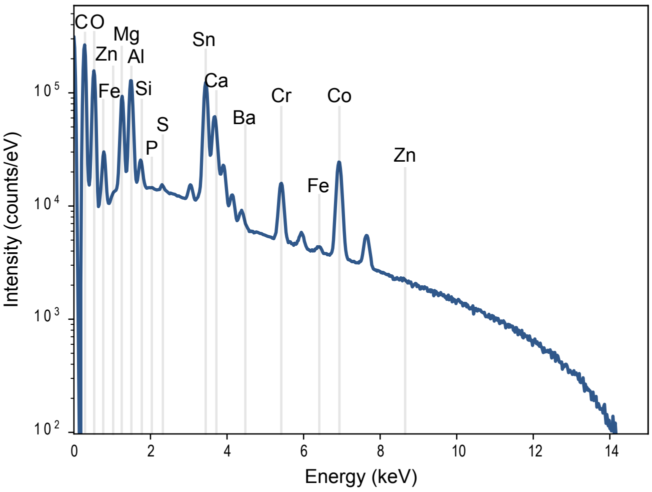

Element	A	Net	Mass. [%]	Atom. [%]
C	6	1142357	47	62
O	8	668804	27	27
Al	13	622968	5	3
Sn	50	1331751	20	3
Mg	12	401085	4	2
Co	27	191401	7	2
Cr	24	91597	2	1
Si	14	61871	0	0
S	16	10534	0	0
Fe	26	4166	0	0
Zn	30	627	0	0
P	15	1219	0	0

LF-O-MB

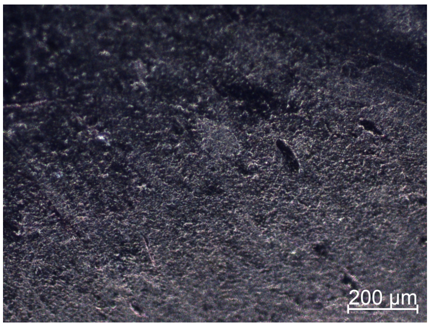

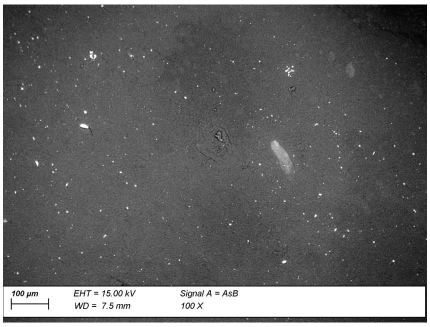

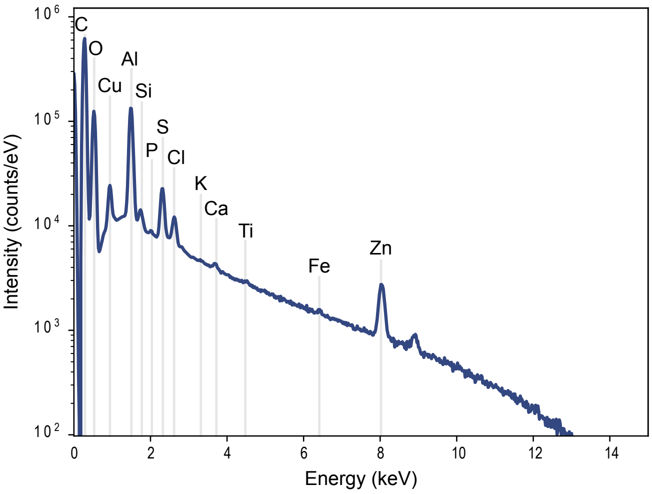

Element	A	Net	Mass. [%]	Atom. [%]
C	6	2622767	68	76
O	8	560994	25	21
Al	13	654418	4	2
Cu	29	18606	1	0
S	16	95989	1	0
Cl	17	38554	0	0
Si	14	25057	0	0
Ca	20	3743	0	0
P	15	2987	0	0
Fe	26	657	0	0
Ti	22	1005	0	0
K	19	1161	0	0

LF-O-UB

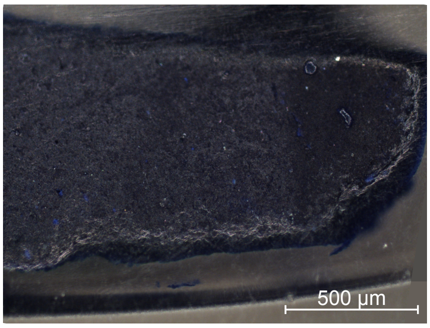

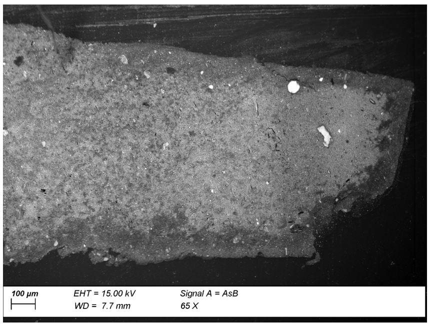

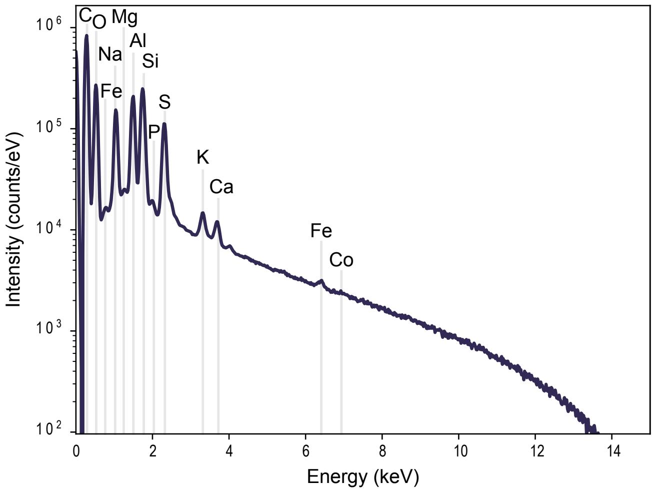

Element	A	Net	Mass. [%]	Atom. [%]
C	6	3661642	76	71
O	8	1258870	32	23
Si	14	1323608	5	2
Na	11	657306	3	2
Al	13	1001140	4	2
S	16	619465	3	1
K	19	42553	0	0
Ca	20	31411	0	0
Mg	12	19909	0	0
P	15	22708	0	0
Cl	17	11472	0	0
Fe	26	3531	0	0
Co	27	630	0	0

LB-O-FW

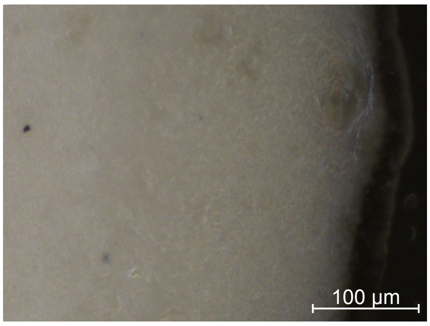

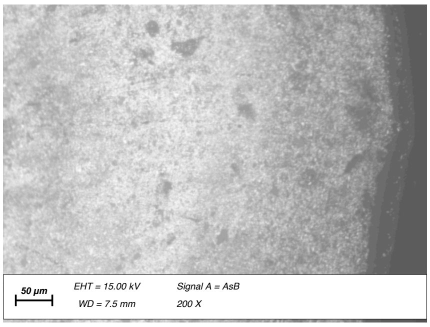

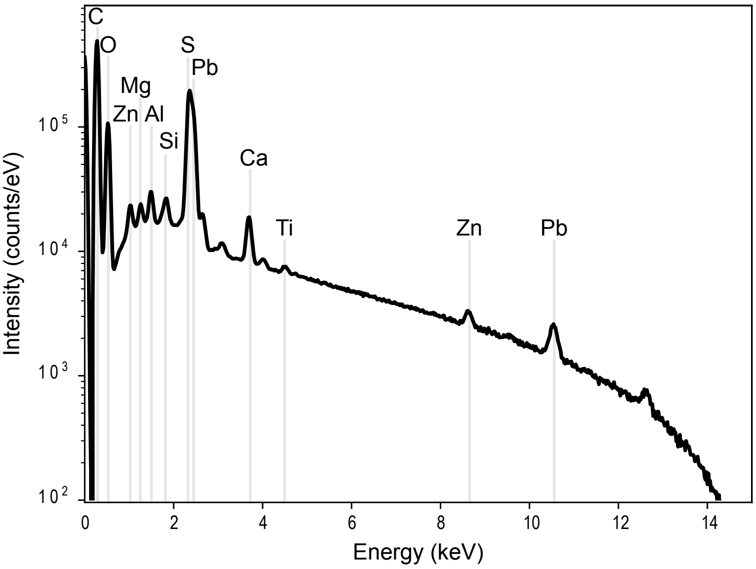

Element	A	Net	Mass. [%]	Atom. [%]
C	6	2126117	53	75
O	8	471577	20	21
Pb	82	1700992	28	2
Ca	20	77860	1	0
Al	13	66374	1	0
Mg	12	33460	0	0
Zn	30	7448	1	0
Ti	22	6051	0	0
Si	14	8590	0	0
S	16	0	0	0

V-O-BC

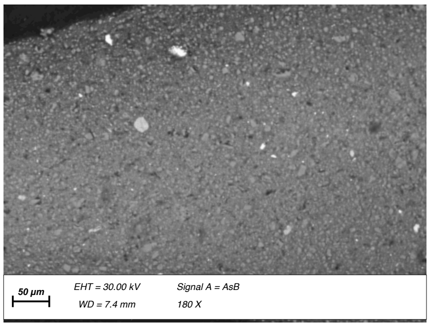

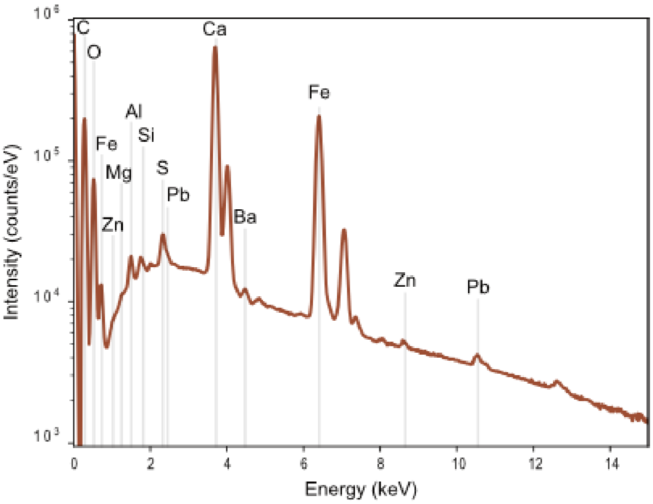

Element	A	Net	Mass. [%]	Atom. [%]
C	6	832540	48	59
O	8	339591	33	31
Ca	20	4695538	18	7
Fe	26	1803504	13	4
Pb	82	15361	1	0
Al	13	38506	0	0
S	16	48291	0	0
Ba	56	24885	0	0
Si	14	27314	0	0
Zn	30	4303	0	0
Mg	12	4855	0	0
P	15	6063	0	0

V-O-JJ

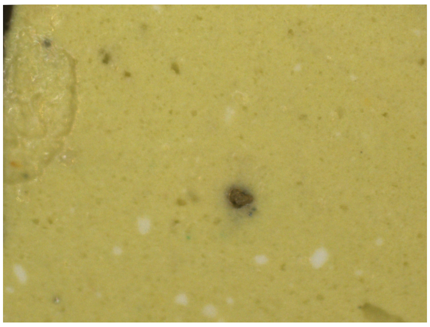

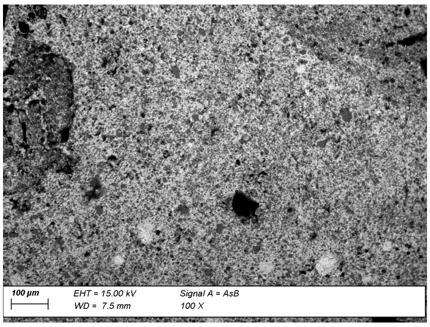

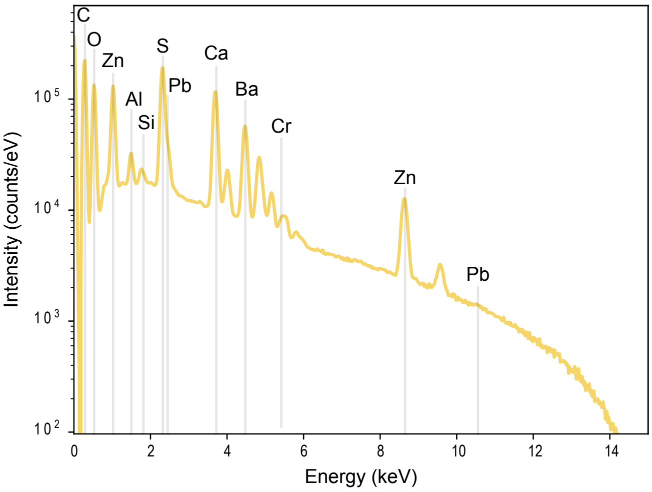

Element	A	Net	Mass. [%]	Atom. [%]
C	6	929403	36	61
O	8	548180	19	25
Ca	20	794944	9	4
S	16	940189	7	4
Zn	30	101984	9	3
Ba	56	656417	14	2
Al	13	79300	1	0
Pb	82	299215	4	0
Cr	24	19868	0	0
Si	14	28494	0	0
Mg	12	5665	0	0
Cl	17	3801	0	0
P	15	1276	0	0
K	19	0	0	0

S8 Additional results of the X-ray diffraction analysis

The crystal phases present in all samples allowed for the identification of pigments and extenders. LF-O-CdYO and LF-O-CdYM both contained CdS mixed with $BaSO_4$, an extender used to reduce costs of Cd based paints starting from the early 20th century [53]. Cd based paints are known to contain ZnO or $Cd_xHg_{1-x}S$ [53], but these phases were not identified. The presence of mineral phases such $CdSO_4 \cdot nH_2O$, CdC_2O_4, attributed to photo degradation reactions were also not identified. Neither were reagents which give hints to the manufacturing process used (dry versus wet [53]), e.g., $CdCO_3$ as reported for early 20th century paint tubes and on paintings [54, 55]. Two samples, LF-O-PGD4 and LF-O-PGD16, were of the same paint designation, but the latter was fabricated at a later time period. XPRD analysis showed that crystal phases in both samples were predominately potassium zinc chromium oxide hydrate, $K_2Zn_4O(CrO_4)_4 \cdot 3\,H_2O$. The diffractograms were obtained by SR-µ-XRD, which exploited minor phases, such as Cr oxide phases, including CrO_3.

S8.1 X-ray diffraction diagrams

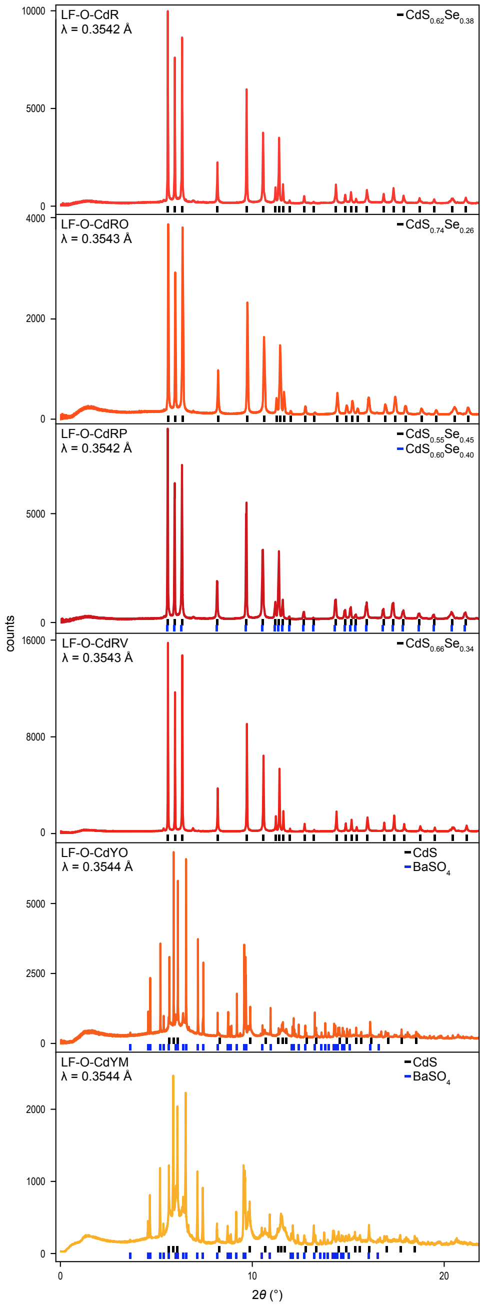

Figure S8.1: XRD diffractograms for samples LF-O-CdX (X = R, RO, RP, RV, O, YM).

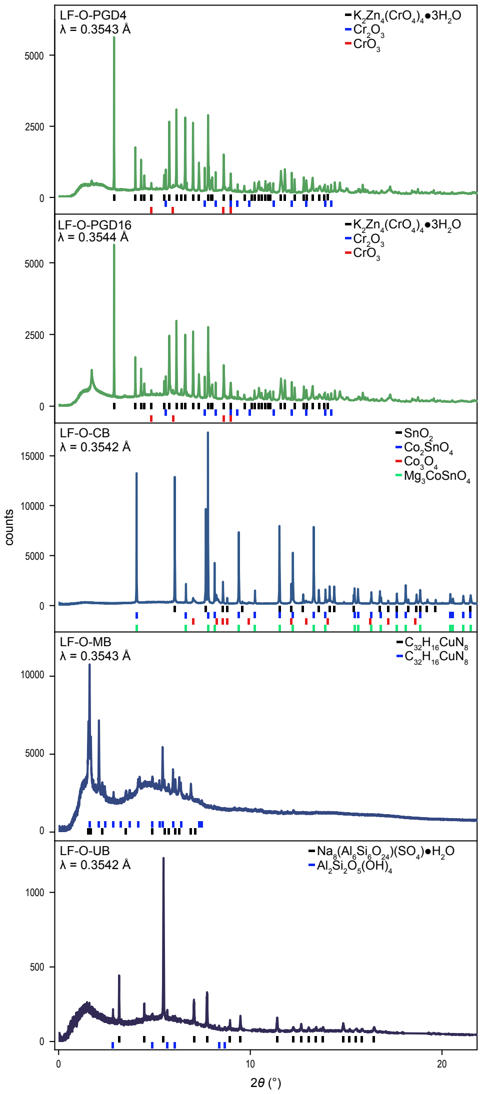

Figure S8.2: XRD diffractograms for LF-O-X (X = PGD4, PGD16, CB, MB, UB).

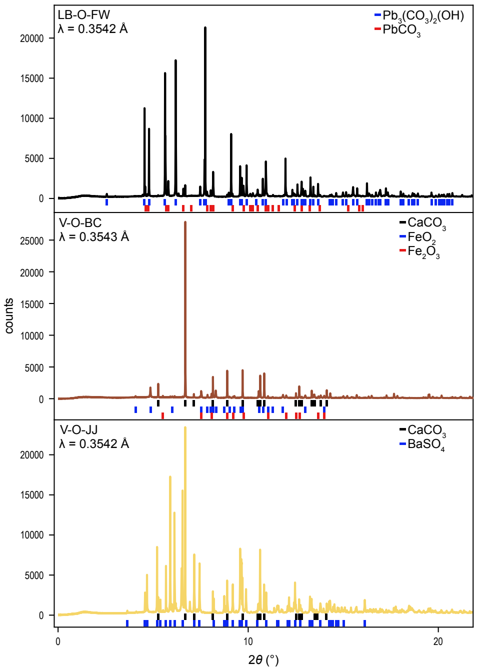

Figure S8.3: XRD diffractograms for LB-O-FW, V-O-JJ, and V-O-BC.

S8.2 Estimation of the selenium content in CdS$_x$Se$_{1-x}$ pigments

The content in selenium of each Cd-based pigment was determined by considering the linear relationship between the d value along the (100) crystal axis and the relative content in Se (noted as x_{Se}). We therefore carefully selected twelve CdS$_x$Se$_{1-x}$ entries of various selenium content from the International Centre for Diffraction Data (ICDD) database (entries: 01-074-9663, 00-041-1049, 00-040-0837, 00-049-1459, 04-020-5584, 00-049-1460, 01-079-5203, 04-002-1185, 04-008-6544, 00-050-0720, 00-050-0721, and 04-011-9599). During this process, low-quality data and data sets collected under non-ambient conditions were discarded. A good linear correlation was then observed (Fig. S8.4). We then estimated $x_{\mathrm{Se}} = 1 - x = [\mathrm{Se}]/[\mathrm{Cd}]$ for all our phases based on this linear correlation, from the position of the d_{100} peak determined using our high angular resolution synchrotron XRD data (Tab. S8.1). Note that the value of x (not x_{Se}) is shown in the tables, according to the usual convention. For LF-O-CdRP, two peaks were observed, indicating two crystalline phases that differ in their S and Se content, with distinct d_{100} values. The estimation in the Se content for both phases are listedis indicated in Tab. S8.1 as "LF-O-CdRP, phase 1" ($x \approx 0.55$, $x_{\mathrm{Se}} \approx 0.45$) and "LF-O-CdRP, phase 2" ($x \approx 0.60$, $x_{\mathrm{Se}} \approx 0.40$).

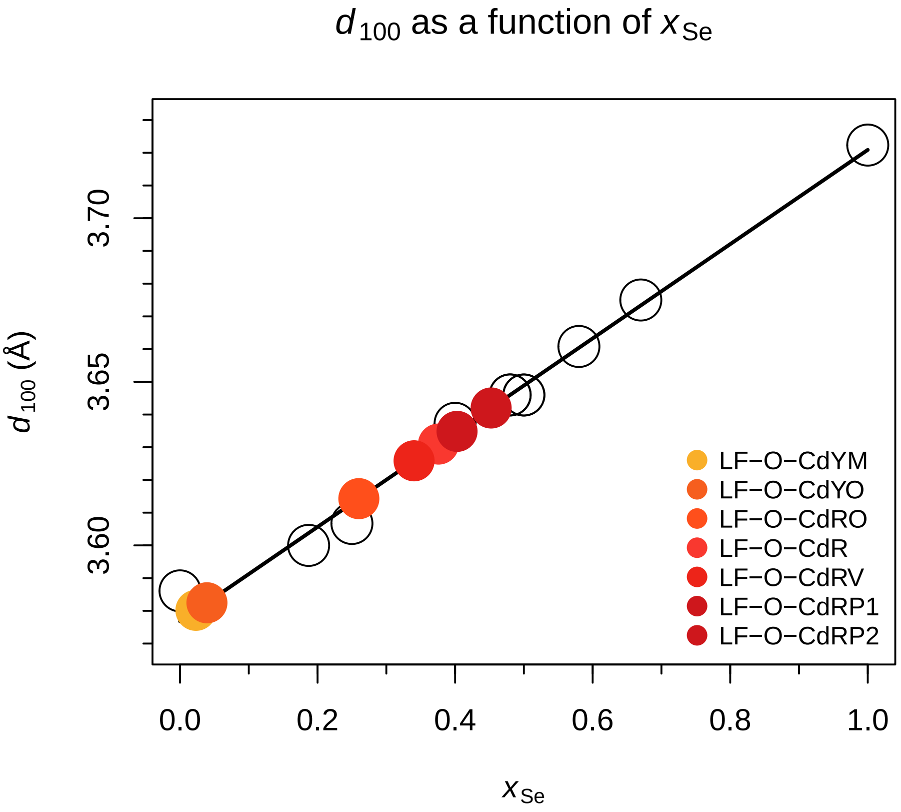

Figure S8.4: Estimation of the selenium content in the Lefebvre-Foinet cadmium-based paint samples. The white points correspond to twelve CdS$_x$Se$_{1-x}$ reference crystal phase entries from the ICDD database. The line represents the best linear fitting of this reference data. The coloured dots correspond to our seven samples, for which the symbol shows the colour of the paint.

Table S8.1: Determination of the content in selenium of the CdS_xSe_{1-x} pigments.

Designation	d_{100} **(Å)**	$x_{\mathbf{Se}}$	$x = 1 - x_{\mathbf{Se}}$
LF-O-CdYM	3.580	0.02	0.98
LF-O-CdYO	3.582	0.04	0.96
LF-O-CdRO	3.614	0.26	0.74
LF-O-CdR	3.631	0.38	0.62
LF-O-CdRV	3.626	0.34	0.66
LF-O-CdRP, phase 1	3.642	0.45	0.55
LF-O-CdRP, phase 2	3.635	0.40	0.60

S9 Summary of the main results obtained

Table S9.1: Main analytical results on the paint composition of the Lefebvre-Foinet paint tubes. MS: metal soaps; PUFA: polyunsaturated fatty acids; FFA: free fatty acids; FMS free metal soaps

Commercial designation	Est. Date	Microscopic morphology	Elemental and structural composition	Molecular composition
Rouge de Cadmium [Cadmium Red]	1969–71	**LF-O-CdR-CS** Two layers: (1) bright red, $\sim$265 µm layer corresponds to exterior surface of LF-O-CdR which was most exposed to air, (2) dark red, in the rest of CS, corresponds interior bulk of LF-O-CdR, which had been less exposed to air; both layers contain bright red aggregates ranging 4–28 µm diameter, <5 µm dark gray grains mostly localized in layer 2, and $\sim$20 µm colorless grains (OM).	**LF-O-CdR-CS** Binder containing <1 µm grains of CdS_xSe_{1-x} dispersed heterogeneously: (1) separates into (1a) concentrated in Cd, S, and Se, $\sim$75 µm thick, and (1b) concentrated in C, $\sim$200 µm thick, (2) concentrated in Cd, S, Se; Cd-containing organics in all layers, Al oxides ranging, 6–40 µm diameter, localized between 1b and 2; traces of Mg, P, Si, and Ti localized in 1a and 2, Zn mostly in 2 (SEM-EDX). **LF-O-CdR** Cadmium sulfide selenide CdS_xSe_{1-x} ($x \approx 0.62$) (H) (SR-µ-XRD).	**LF-O-CdR** Linseed oil (HPLC). Polymeric network present (Py-GC-MS). Low oxidation, advanced stage in curing, but PUFA still present and abundant (linoleic acid); FFA and FMS: present, MS have formed with the oil (azelaic acid); given the similar profile of FFA and FMS+FFA, we cannot conclude on the addition of FFA nor FMS (GC-MS). C=C still present at $1630\,\mathrm{cm}^{-1}$; broad band with weak shoulders in the carboxylate region, carboxylates present, but impossible to identify the species; oxalates formed (FT-IR).
Rouge de Cadmium Orange [Cadmium Red Orange]	1962–63	**LF-O-CdRO-CS** Two layers: (1) lighter red-orange, reflective, $\sim$215 µm zone in center of CS from hole in LF-O-CdRO, possibly covered in resin during CS prep or dried zone, (2) darker red-orange, matte in rest of CS; both layers contain $\sim$6 µm red grains, and $\sim$21 µm dark, gray grains localized between 1 and 2 (OM).	**LF-O-CdRO-CS** Binder containing small grains of CdS_xSe_{1-x} <1 µm dispersed heterogeneously: (1) concentrated in C, (2) concentrated in Cd, S, Se; Cd-containing organic agglomerates, $\sim$50 µm, localized between 1 and 2, $\sim$10–15 µm Al oxides localized in 2; trace elements in both layers include Si, Ti and Zn (SEM-EDX). **LF-O-CdRO** Cadmium sulfide selenide CdS_xSe_{1-x} ($x \approx 0.74$) (H) (SR-µ-XRD).	**LF-O-CdRO** Linseed oil (HPLC). Polymeric network present (Py-GC-MS). Curing is ongoing, but with high PUFA content (linoleic acid); FFA and FMS: present, MS have formed with oil (azelaic acid); given the similar profile of FFA and FMS+FFA, we cannot conclude on the addition of FFA nor FMS (GC-MS). Crystalline & amorphous Zn-carboxylates, Cd-carboxylates; as Zn does not appear to belong to the coloring matter, we may hypothesize the addition of Zn soaps; oxalates formed (FT-IR).

Continued on next page

Table S9.1: Main analytical results on the paint composition of the Lefebvre-Foinet paint tubes. MS: metal soaps; PUFA: polyunsaturated fatty acids; FFA: free fatty acids; FMS free metal soaps (Continued)

Commercial designation	**Est. Date**	**Microscopic morphology**	**Elemental and structural composition**	**Molecular composition**
Rouge de Cadmium Pourpre [Cadmium Red Purple]	1958–59	**LF-O-CdRP-CS** Dark, red paint of contrasting shades; light red agglomerates ranging 3–70 µm diameter, larger agglomerates in center of CS; colorless grains ranging 25–50 µm diameter, dark gray grains <5 µm diameter (OM).	**LF-O-CdRP-CS** Binder containing <1 µm grains of CdS_xSe_{1-x} dispersed heterogeneously. $\sim$50 µm Ca-containing organic agglomerate 2–10 µm Al oxides, a $\sim$10 µm grain concentrated in Fe; trace elements include P, Si, and Zn (SEM-EDX). **LF-O-CdRP** Cadmium sulfide selenide CdS_xSe_{1-x} ($x \approx 0.55, 0.60$) (H) (SR-µ-XRD).	**LF-O-CdRP** Mixture of linseed and safflower oils, with beeswax esters (HPLC). Polymeric network detected, although relatively lower degree of polymerization with respect to other Cd based paints, in agreement with the presence of safflower oil (Py-GC-MS). Advanced oxidation, in agreement with the presence of safflower oil, which is prone to oxidative degradation; curing is ongoing, with PUFA still present (linoleic acid); FFA and FMS: present, MS have formed with the oil (azelaic acid); given the similar profile of FFA and FMS+FFA, we cannot conclude on the addition of FFA nor FMS (GC-MS). Crystalline & amorphous Zn-carboxylates, Cd-carboxylates; as Zn does not appear to belong to the coloring matter, we may hypothesize the addition of Zn soaps (FT-IR).

Continued on next page

Table S9.1: Main analytical results on the paint composition of the Lefebvre-Foinet paint tubes. MS: metal soaps; PUFA: polyunsaturated fatty acids; FFA: free fatty acids; FMS free metal soaps (Continued)

Commercial designation	**Est. Date**	**Microscopic morphology**	**Elemental and structural composition**	**Molecular composition**
Rouge de Cadmium Vermillon [Cadmium Red Vermilion]	1963	**LF-O-CdRV-CS** Four zones: (1) dark red in center of CS corresponds to bulk material, (2) lighter red, reflective, ∼175 µm from edge to center, along border of CS, hypothesized to be from a hole in CS either covered in resin during CS prep or dried, (3) darker red, ∼100 µm thick along upper edge of CS, (4) light red, matte zone ∼160 µm diameter, from edge of CS to bulk of sample; layers 1–3 contain ∼6 µm red grains and ∼5 µm dark grains (OM).	**LF-O-CdRV-CS** Binder containing small grains of CdS_xSe_{1-x} <1 µm localized mostly in 1, at lower concentration in 2, Al oxide particles localized in 2 and 3, layers 2–4 concentrated in C; traces of Si, P and Zn localized in 1 (SEM-EDX). **LF-O-CdRV** Cadmium selenide Sulfide CdS_xSe_{1-x} ($x \approx 0.66$) (H) (SR-µ-XRD).	**LF-O-CdRV** Linseed oil (HPLC). Polymeric network present (Py-GC-MS). Low oxidation, curing is ongoing, with PUFA still present (linoleic acid); FFA and FMS: present, MS have formed with the oil (azelaic acid); given the similar profile of FFA and FMS+FFA, we cannot conclude on the addition of FFA nor FMS (GC-MS). C=C still present at $1630\,cm^{-1}$; crystalline & amorphous Zn-carboxylates, Cd-carboxylates; as Zn does not appear to belong to the coloring matter, we may hypothesize the addition of Zn soaps (FT-IR).
Orange de Cadmium Jaune [Cadmium Yellow Orange]	1963	**LF-O-CdYO-CS** Homogeneous bright orange, reflective surface, red agglomerates ∼5 µm, dark, gray shiny agglomerates ∼5–10 µm, black particles ∼5 µm (OM).	**LF-O-CdYO-CS** Binder containing <1 µm grains of CdS dispersed heterogeneously, ∼2 µm agglomerates concentrated in Ba and S, ∼10 µm Al oxides, ∼25 µm Ca oxide grains, and zones concentrated in C corresponding to higher binder concentration; trace elements include of Fe and Zn localized in Cd-concentrated zones, Mg localized in Ca zones, and Si (SEM-EDX). **LF-O-CdYO** Cadmium sulfide CdS (H), Barium sulfate $BaSO_4$ (O) (SR-µ-XRD).	**LF-O-CdYO** Linseed oil (HPLC). Polymeric network present (Py-GC-MS). Low oxidation, curing is taking place; FFA and FMS: present, MS have formed with the oil (azelaic acid); given the similar profile of FFA and FMS+FFA, we cannot conclude on the addition of FFA nor FMS (GC-MS). C=C still detected at $1630\ cm^{-1}$; broad band with weak shoulders in the carboxylate region; $BaSO_4$ (FT-IR).

Continued on next page

Table S9.1: Main analytical results on the paint composition of the Lefebvre-Foinet paint tubes. MS: metal soaps; PUFA: polyunsaturated fatty acids; FFA: free fatty acids; FMS free metal soaps (Continued)

Commercial designation	**Est. Date**	**Microscopic morphology**	**Elemental and structural composition**	**Molecular composition**
Jaune de Cadmium Moyen [Cadmium Yellow Medium]	1962–63	**LF-O-CdYM-CS** Yellow, with reflective surface, appearing relatively homogeneous (1), red particles ∼5 µm dispersed throughout 2, black particles ∼5 µm (3), colorless particles ∼5–10 µm (4), dark gray, shiny particles ∼5 µm (5) (OM).	**LF-O-CdYM-CS** (1) Binder containing <1 µm grains of CdS dispersed heterogeneously, mixed with small particles of $BaSO_4$, Al oxides, Si particles as 5; trace elements dispersed in 1 include Zn, Ti and P (SEM-EDX). **LF-O-CdYM** Cadmium sulfide CdS (H), Barium sulfate $BaSO_4$ (O) (SR-µ-XRD).	**LF-O-CdYM** Linseed oil (HPLC). Polymeric network present (Py-GC-MS). Curing is ongoing with PUFA still present (linoleic acid); mostly FFA, small amount of FMS (GC-MS). C=C still detected at $1630\,cm^{-1}$, $BaSO_4$, unassigned peak at $1570\,cm^{-1}$ (FT-IR).
Vert Permanent Foncé (4) [Permanent Green Deep]	1963–65	**LF-O-PGD4-CS** Dark green crystals ranging 10–515 µm diameter (1), reflecting grains (2) on surface, dispersed in dark green (3), light green (4), and yellow particles (5) (OM).	**LF-O-PGD4-CS** Cr oxide crystals (1) with pure Cr (2) from 10–515 µm in binder containing and <1 µm Cr grains (3), mixed with Zn and K corresponding to 4 and 5; trace elements include Al, Ba, Ca, Cl, S, P, Si, Cl and Ti (SEM-EDX). **LF-O-PGD4** Potassium zinc chromium oxide hydrate $K_2Zn_4O(CrO_4)_4 \cdot 3\,(H_2O)$, Chromium oxide Cr_2O_3, Chromium oxide CrO_3 (SR-µ-XRD).	**LF-O-PGD4** Linseed oil (HPLC). Polymeric network present (Py-GC-MS). MS have formed with the oil (azelaic acid); Low oxidation, curing is ongoing with PUFA still present (linoleic acid); FFA and FMS: present, MS have formed with the oil (azelaic acid); given the similar profile of monocarboxylic FFA and FMS+FFA, we cannot conclude on the addition of FFA nor FMS (GC-MS). Crystalline & amorphous Zn-carboxylates; unassigned peak at $1546\,cm^{-1}$, may come from the metal carboxylates as additive; CrO_3 (FT-IR).

Continued on next page

Table S9.1: Main analytical results on the paint composition of the Lefebvre-Foinet paint tubes. MS: metal soaps; PUFA: polyunsaturated fatty acids; FFA: free fatty acids; FMS free metal soaps (Continued)

Commercial designation	**Est. Date**	**Microscopic morphology**	**Elemental and structural composition**	**Molecular composition**
Vert Permanent Foncé (16) [Permanent Green Deep]	1970–72	**LF-O-PGD16-CS** Dark and medium green crystals ranging 3–30 µm diameter (1), dispersed in <1 µm light green grains (2), with zones of <1 µm yellow-green grains (3), dark yellow, transparent grains ranging 2–40 µm diameter (4), and <1 µm colorless crystals (5); hollowed border of $\sim$140 µm around half of CS (6) (OM).	**LF-O-PGD16-CS** Binder containing 50 µm Cr oxide crystals (1) and <1 µm Cr grains (2), mixed with <1 µm Zn and K grains (2), (3) and (4) dispersed heterogeneously. (6) concentrated in C containing Cr particles ranging 5–35 µm; trace elements include Ca, Cd, Cl, Co, Fe, S, Si, and Ti (SEM-EDX). **LF-O-PGD16** Potassium zinc chromium oxide hydrate $K_2Zn_4O(CrO_4)_4 \cdot 3\,(H_2O)$, Chromium oxide Cr_2O_3, Chromium oxide CrO_3 (SR-µ-XRD).	**LF-O-PGD16** Linseed oil + safflower oil (HPLC). Polymeric network present (Py-GC-MS). Advanced oxidation, advanced curing, much more oxidized than LF-O-PGD4, in agreement with the presence of safflower oil, which is prone to oxidative degradation; FFA and FMS: present, relatively high degree of saponification, MS have formed with the oil (azelaic acid); given the similar profile of monocarboxylic FFA and FMS+FFA, we cannot conclude on the addition of FFA nor FMS (GC-MS). Bridge-like band, difficult to confirm the presence nor the species of carboxylates; CrO_3 (FT-IR).

Continued on next page

Table S9.1: Main analytical results on the paint composition of the Lefebvre-Foinet paint tubes. MS: metal soaps; PUFA: polyunsaturated fatty acids; FFA: free fatty acids; FMS free metal soaps (Continued)

Commercial designation	Est. Date	Microscopic morphology	Elemental and structural composition	Molecular composition
Bleu Coeruleum [Cerulean Blue]	1966–67	**LF-O-CB-CS** Two zones: (1) lighter blue around edges of CS corresponds to surface of LF-O-CB, most exposed to air, (2) darker blue in center of CS corresponds to bulk of LF-O-CB and contains dark blue grains ranging 2–20 µm (OM).	**LF-O-CB-CS** Binder containing <1 µm grains of $CoO \cdot xSnO_2$ dispersed heterogeneously; trace elements include Mg, Al, Cr, Si, P, S, Fe, Na; SEM shows contrasting zones, but elemental mapping shows relatively homogeneous distribution of elements (SEM-EDX). **LF-O-CB** Tin oxide SnO_2 (T), Cobalt tin oxide Co_2SnO_4 (C), Cobalt oxide Co_3O_4 (C), Cobalt magnesium tin oxide $Mg_{1.61}Co_{0.39}SnO_4$ (C) (SR-µ-XRD).	**LF-O-CB** Linseed oil (HPLC). Polymeric network present (Py-GC-MS). Relatively high degree of hydrolysis, advanced oxidation, advanced curing; FFA and FMS: present, MS have formed with the oil (azelaic acid); given the similar profile of FFA and FMS+FFA, we cannot conclude on the addition of FFA nor FMS (GC-MS). C=C still detected at $1630\,cm^{-1}$; split carbonyl absorption band appearing as a doublet at $\sim 1740/1710\,cm^{-1}$ (confirming higher degree of oxidation and hydrolysis); bridge-like band, difficult to confirm the presence nor the species of carboxylates; oxalates formed (FT-IR).

Continued on next page

Table S9.1: Main analytical results on the paint composition of the Lefebvre-Foinet paint tubes. MS: metal soaps; PUFA: polyunsaturated fatty acids; FFA: free fatty acids; FMS free metal soaps (Continued)

Commercial designation	**Est. Date**	**Microscopic morphology**	**Elemental and structural composition**	**Molecular composition**
Bleu Monacal [Monacal Blue]	1979	**LF-O-MB-CS** Homogeneous dark blue paint with colorless grains ranging 10–75 µm (OM).	**LF-O-MB-CS** Binder containing small grains <1 µm; trace elements of Al, Si, P, S, Cl, K, Ca and Cu; SEM shows contrasting zones, but elemental mapping shows relatively homogeneous distribution of elements (SEM-EDX). **LF-O-MB** Copper phthalocyanine $C_{32}H_{16}CuN_8$, β-Copper phthalocyanine $C_{32}H_{16}CuN_8$ (SR-µ-XRD).	**LF-O-MB** Linseed oil (HPLC). Polymeric network present (Py-GC-MS). Relatively high degree of hydrolysis, low oxidation, curing is ongoing, with PUFA still present (linoleic acid); FFA and FMS: present (GC-MS). Bridge-like band, difficult to identify the species of carboxylates, unassigned peak at 1507 cm^{-1}, may come from the metal carboxylates as additive; split carbonyl absorption band appearing as a doublet at $\sim$1740/1710 cm^{-1} (confirming higher degree of hydrolysis) (FT-IR).

Continued on next page

Table S9.1: Main analytical results on the paint composition of the Lefebvre-Foinet paint tubes. MS: metal soaps; PUFA: polyunsaturated fatty acids; FFA: free fatty acids; FMS free metal soaps (Continued)

Commercial designation	**Est. Date**	**Microscopic morphology**	**Elemental and structural composition**	**Molecular composition**
Bleu Outremer [Ultramarine Blue]	1970–72	**LF-O-UB-CS** Three layers: (1) dark blue 500 µm starting from edge of CS, corresponds to LF-O-UB most exposed to air, (2) lighter dark blue than 1, intermediate layer 630 µm starting from 1 to 3 lighter dark blue than 2, rest of CS corresponds to bulk of LF-O-UB, least exposed to air; bright blue 10 µm zones observed which appear to be under surface of CS, in bulk of LF-O-UB (OM).	**LF-O-UB-CS** Binder containing small grains <1 µm of Na, Al, Si, dispersed heterogeneously: (1) concentrated in Na, Al, Si, (2) separated into (2a) C-concentrated and (2b) concentrated in Na, Al, Si, (3) C-concentrated and (4) C-concentrated border along entire CS 60–65 µm and appears hollowed; agglomerates of ∼25 µm Al oxides in all layers, and ∼35 µm Ca-concentrated particles in 1 and 5; SEM shows contrasting zones, but elemental analysis does not clearly distinct which correspond; trace elements include Mg, P, S, Cl, K and Fe (SEM-EDX). **LF-O-UB** Sodium aluminum silicate sulfate hydrate $Na_{8.08}(Al_6Si_6O_{24})(SO_4)_{0.98}(H_2O)_{0.96}$ (C), Aluminum silicate hydroxide $Al_2Si_2O_5(OH)_4$ (A) (SR-µ-XRD).	**LF-O-UB** Linseed oil with beeswax ethers (HPLC). Polymeric network present (Py-GC-MS). High degree of hydrolysis, low oxidation, relatively advanced stage of curing given the lowest amount of unreacted double bonds; FFA and FMS: present, MS have formed with oil (azelaic), given the similar profile of FFA and FMS+FFA, we cannot conclude on the addition of free fatty acids nor metal soaps (GC-MS). Bridge-like band, difficult to identify the species of carboxylates; silicate bands confirmed the presence of ultramarine blue pigment (FT-IR).

Table S9.2: Main analytical results on the paint composition of the Lefranc & Bourgeois paint tube. MS: metal soaps; PUFA: polyunsaturated fatty acids; FFA: free fatty acids; FMS free metal soaps

Commercial designation	**Est. Date**	**Microscopic morphology**	**Elemental and structural composition**	**Molecular composition**
Blanc d'Argent [Flake White]	1987–90	**LB-O-FW-CS** Three layers: (1) yellow, transparent, 25 µm starting from edge of CS corresponds to LB-O-FW most exposed to air, (2) white-yellow, intermediate layer, 250 µm from 1 to 3, (3) white paint, rest of CS corresponds to bulk LB-O-FW which was least exposed to air (OM).	**LB-O-FW-CS** Binder containing <1 µm grains of $PbCO_3$ heterogeneously dispersed: (1) C-concentrated with<1 µm Pb particles, (2) Pb-concentrated, with a gradient of increasing concentration from 1 to 3, (3) Pb-concentrated, containing ∼10 µm Ca oxides and ∼15 µm Al oxides localized between 2 and 3; trace elements include Si, Ti, and Zn in 2 and 3 (SEM-EDX). **LB-O-FW** Hydrocerussite $Pb_3(CO_3)_2(OH)_2$ (R), Cerussite $PbCO_3$ (O) (SR-µ-XRD).	**LB-O-FW** Linseed oil (HPLC). Polymeric network present (Py-GC-MS). Low oxidation, curing is ongoing; FFA and FMS: high degree of saponification, with negligible FFA and high content of FMS, which have formed with the oil (azelaic acid) (GC-MS). $C{=}C$ still detected at $1630\,cm^{-1}$; $CaCO_3$; Pb-carboxylate expected but not unambiguously identified, possibly concealed by the broad band in carboxylate region; amorphous Zn-carboxylate detected (FT-IR).

Table S9.3: Main analytical results on the paint composition of the Valor paint cans. MS: metal soaps; PUFA: polyunsaturated fatty acids; FFA: free fatty acids; FMS free metal soaps

Commercial designation	**Est. Date**	**Microscopic morphology**	**Elemental and structural composition**	**Molecular composition**
Bois Clair	1958(?)	**V-O-BC-CS** Two layers: (1) brown, 150 µm from edge to bulk and surrounding entire CS, corresponds to V-O-BC most exposed to air and (2) dark brown, corresponds to bulk of V-O-BC least exposed to air; both layers contain ∼10 µm black particles, ∼5 µm red particles, and ∼20 µm colorless grains (OM).	**V-O-BC-CS** Binder containing <1 µm grains of Fe and Ca, agglomerates concentrated in Ca ranging 2–19 µm, <1 µm grains of Pb, ∼10–15 µm agglomerates concentrated in Ba and S ∼10 µm Al-concentrated agglomerates and ∼10 µm Si-concentrated agglomerates; trace elements include of P, Mg, Zn, and Cu (SEM-EDX). **V-O-BC** Iron dioxide FeO_2, Ferric oxide Fe_2O_3, Calcite $CaCO_3$ (SR-µ-XRD).	**V-O-BC** Linseed oil (HPLC). Polymeric network not detected, probably due to a phase separation occurring in the can (Py-GC-MS). Advanced oxidation, curing ongoing; FFA and small amounts of FMS: detected, MS have formed with oil (azelaic acid); given the similar profile of FFA and MS+FFA, we cannot conclude on the addition of FFA nor FMS; *Pinaceae* resin detected (GC-MS). Bridge-like band, difficult to identify the species of carboxylates; strong signals of $CaCO_3$ (FT-IR).
Jaune de Jonquille	1963 or 1966-67	**V-O-JJ-CS** Light yellow paint (1) containing white particles ranging 14–44 µm (2), ∼13 µm colorless grains (3), ∼30 µm, dark yellow zone (4), ∼57 µm brown-green agglomerate (5), and ∼6 µm green grains (6) (OM).	**V-O-JJ-CS** Binder containing <1 µm grains Zn, S, Si and Pb corresponds to (1), particles concentrated in Ba and S (2), particles concentrated in Ca and Al (3), zone concentrated in Pb and S (4), and particle concentrated in C (5); traces of Mg and P (SEM-EDX). **V-O-JJ** Calcite $CaCO_3$ (R), Barium sulfate $BaSO_4$ (O) (SR-µ-XRD).	**V-O-JJ** Linseed oil (HPLC). Polymeric network not detected (Py-GC-MS). Relatively high degree of hydrolysis, low oxidation, slow curing with PUFA still present (linoleic acid, linolenic acid); FFA and FMS: present; *Pinaceae* resin detected (GC-MS). Crystalline Zn-carboxylates, Pb-carboxylates $BaSO_4$; strong signals of $CaCO_3$ (FT-IR).

References

[1] M. Warnock, Simon Hantaï, Transatlantique, ER Publishing, New York, 2021.

[2] O. D. Odita, The Mark and Making in the Work of Simon Hantaï, in: Simon Hantaï, Transatlantique, ER Publishing, 2021, pp. 16–19.

[3] A. Baldassari, ”He lived in his painting” Interview with Zsuzsa Hantaï, in: Simon Hantaï The Centenary Exhibition, Fondation Louis Vuitton, Gallimard, Paris, 2022, pp. 18–30, 978-2-07-297988-0.

[4] M. Warnock, Penser la peinture: Simon Hantaï, Art et artistes, Gallimard, Paris, 2012.

[5] S. Crowner, Hantaï: Color, Shape, Indecision, Decision, La Marche du Crabe, in: M. Warnock (Ed.), Simon Hantaï, Transatlantique, ER Publishing, 2021, pp. 26–31.

[6] A. Baldassari, A Story of a Life: Simon Hantaï, 1922-2008, in: Simon Hantaï The Centenary Exhibition, Fondation Louis Vuitton, Gallimard, Paris, 2022, pp. 90–139, 978-2-07-297988-0.

[7] A. Pacquement, I. Monod-Fontaine, D. Fourcade, 1982: Simon Hantaï Withdraws, in: Simon Hantaï: exposition, Paris, Centre Pompidou, Galerie 1, 22 mai - 9 septembre 2013, Centre Pompidou, Paris, 2013, pp. 201–209, 978-2-84426-599-9.

[8] J. Ault, Simon Hantaï's Active Silence, in: Simon Hantaï, Transatlantique, ER Publishing, 2021, pp. 32–41.

[9] G. Didi-Huberman, L'étoilement. Conversation avec Hantaï, Éditions de Minuit, Paris, 1998.

[10] J. J. Boon, F. G. Hoogland, Investigating Fluidizing Dripping Pink Commercial Paint on Van Hemert's Seven-Series Works from 1990–1995, in: K. J. van den Berg, A. Burnstock, M. de Keijzer, J. Krueger, T. Learner, A. Tagle, de, G. Heydenreich (Eds.), Issues in Contemporary Oil Paint, Springer International Publishing, Cham, 2014, pp. 227–246, 978-3-319-10100-2. `doi:10.1007/978-3-319-10100-2_16`.
URL `http://link.springer.com/10.1007/978-3-319-10100-2_16`

[11] M.-C. Corbeil, K. Helwig, J. Poulin, Jean Paul Riopelle: The Artist's Materials, 1st Edition, Getty Conservation Institute, Los Angeles, 2011.

[12] Gifted Art Foundation, Mondrian Route: Lefebvre-Foinet (2020).
URL `https://www.mondrianroute.com/areas/paris/winkel-lefebvre-foinet`

[13] Sites & Monuments, Sites et monuments : bulletin de la Société pour la protection des paysages et de l'esthétique générale de la France, Société pour la protection des paysages et de l'esthétique de la France (Paris) 150, 1995/07/01 (N150)-1995/09/30. 06/11/2017 Online date: 06/11/2017 Source: Société pour la protection des paysages et de l'esthétique de la France, 2017-98990 (Jul. 1995).

[14] Christie's, Collection Lefebvre-Foinet Art Moderne et d'Après-Guerre (Dec. 2009).
URL `http://www.search-antiques.com/fr/revue-art/2008/Collection%20Lefebvre-Foinet.pdf`

[15] Sites & Monuments, Sites et monuments : bulletin de la Société pour la protection des paysages et de l'esthétique générale de la France, Société pour la protection des paysages et de l'esthétique de la France (Paris) 155, 01 octobre 19961996 /10/01 (N155)- 1996 /12/31. 06/11/2017 Online date: 29/08/2017 (Oct. 1996).

[16] P. Helou de la Grandière, Technique classique et problèmes contemporains: Pierre Soulages, Peinture 114x165, 16 décembre 1959 Musée de l'Art moderne de la Ville de Paris, Ph.D. thesis, Insitut national du patrimoine (Sep. 2005).

[17] F. Casadio, A. Bezúr, I. Fiedler, K. Muir, T. Trad, S. Maccagnola, Pablo Picasso to Jasper Johns: a Raman study of cobalt-based synthetic inorganic pigments, Journal of Raman Spectroscopy 43 (11) (2012) 1761–1771. `doi:10.1002/jrs.4081`.
URL `https://onlinelibrary.wiley.com/doi/10.1002/jrs.4081`

[18] M. Kokkori, F. Casadio, J. J. Boon, A comprehensive study of early 20th-century oil-based enamel paints: Integrating industrial technical literature and analytical data, in: J. Bridgland (Ed.), ICOM-CC 17th triennial conference preprints, Melbourne, 15-19 September 2014, International Council of Museums, Paris, 2014, p. 1519.

[19] L. Bourgeois, Lefranc Bourgeois History (2023).
URL `https://www.lefrancbourgeois.com/row/heritage/history/`

[20] J. Rainhorn, Portraits grinçants de la céruse en assassin dans "L'Assiette au beurre" (1905), Parlement[s], Revue d'histoire politique N°33 (1) (2021) 233. `doi:10.3917/parl2.033.0233`.
URL `http://www.cairn.info/revue-parlements-2021-1-page-233.htm?ref=doi`

[21] L. Lestel, La production de céruse en France au XIXe siècle : évolution d'une industrie dangereuse, Techniques & Culture. Revue semestrielle d'anthropologie des techniques 38, number: 38 Publisher: Les Éditions de l'EHESS (Mar. 2002). `doi:10.4000/tc.1067`.
URL `https://journals.openedition.org/tc/1067`

[22] R. Bécot, Thomas Le Roux (dir.), Risques industriels. Savoirs, régulations, politiques d'assistance, fin XVIIe-début XXe siècle: Rennes, Presses universitaires de Rennes, 2016, 348 p., Histoire Politique (Sep. 2017). `doi:10.4000/histoirepolitique.6890`.
URL `http://journals.openedition.org/histoirepolitique/6890`

[23] L. Beck, Ion Beam Analysis and 14C Accelerator Mass Spectroscopy to Identify Ancient and Recent Art Forgeries, Physics 4 (2) (2022) 462–472. `doi:10.3390/physics4020031`.
URL `https://www.mdpi.com/2624-8174/4/2/31`

[24] J.-P. Dumoulin, C. Comby-Zerbino, E. Delqué-Količ, C. Moreau, I. Caffy, S. Hain, M. Perron, B. Thellier, V. Setti, B. Berthier, L. Beck, Status Report on Sample Preparation Protocols Developed at the LMC14 Laboratory, Saclay, France: From Sample Collection to ^{14} C AMS Measurement, Radiocarbon 59 (3) (2017) 713–726. `doi:10.1017/RDC.2016.116`.
URL `https://www.cambridge.org/core/product/identifier/S0033822216001168/type/journal_article`

[25] L. Beck, C. Messager, S. Coelho, I. Caffy, E. Delqué-Količ, M. Perron, S. Mussard, J.-P. Dumoulin, C. Moreau, V. Gonzalez, E. Foy, F. Miserque, C. Bonnot-Diconne, Thermal Decomposition of Lead White for Radiocarbon Dating of Paintings, Radiocarbon 61 (5) (2019) 1345–1356. `doi:10.1017/RDC.2019.64`.
URL `https://www.cambridge.org/core/product/identifier/S003382221900064X/type/journal_article`

[26] C. Messager, L. Beck, L. d. Viguerie, M. Jaber, Thermal analysis of carbonate pigments and linseed oil to optimize CO2 extraction for radiocarbon dating of lead white paintings, Microchemical Journal 154 (2020) 104637. `doi:10.1016/j.microc.2020.104637`.
URL `https://linkinghub.elsevier.com/retrieve/pii/S0026265X19323732`

[27] C. Moreau, C. Messager, B. Berthier, S. Hain, B. Thellier, J.-P. Dumoulin, I. Caffy, M. Sieudat, E. Delqué-Količ, S. Mussard, M. Perron, V. Setti, L. Beck, ARTEMIS, the 14C AMS facility of the LMC14 national laboratory: a status report on quality control and microsample procedures, Radiocarbon 62 (6) (2020) 1755–1770. `doi:10.1017/RDC.2020.73`.
URL `https://www.cambridge.org/core/product/identifier/S0033822220000739/type/journal_article`

[28] L. Beck, I. Caffy, E. Delqué-Količ, J.-P. Dumoulin, C. Goulas, S. Hain, C. Moreau, M. Perron, V. Setti, M. Sieudat, B. Thellier, 20 years of AMS ^{14}C dating using the ARTEMIS facility at the LMC14 national laboratory: Review of service and research activities, Radiocarbon (2023) 1–13`doi:10.1017/RDC.2023.23`.
URL `https://www.cambridge.org/core/product/identifier/S0033822223000231/type/journal_article`

[29] C. B. Ramsey, S. Lee, Recent and Planned Developments of the Program OxCal, Radiocarbon 55 (2) (2013) 720–730. `doi:10.1017/S0033822200057878`.
URL `https://www.cambridge.org/core/product/identifier/S0033822200057878/type/journal_article`

[30] Q. Hua, J. C. Turnbull, G. M. Santos, A. Z. Rakowski, S. Ancapichún, R. De Pol-Holz, S. Hammer, S. J. Lehman, I. Levin, J. B. Miller, J. G. Palmer, C. S. M. Turney, Atmospheric radiocarbon for the period 1950-2019, Radiocarbon 64 (4) (2022) 723–745. `doi:10.1017/RDC.2021.95`.
URL `https://www.cambridge.org/core/product/identifier/S0033822221000953/type/journal_article`

[31] J. La Nasa, J. Lee, I. Degano, A. Burnstock, K. J. van den Berg, B. Ormsby, I. Bonaduce, The role of the polymeric network in the water sensitivity of modern oil paints, Scientific Reports 9 (1) (2019) 3467. `doi:10.1038/s41598-019-39963-z`.
URL `http://www.nature.com/articles/s41598-019-39963-z`

[32] J. La Nasa, F. Nardella, L. Andrei, M. Giani, I. Degano, M. P. Colombini, E. Ribechini, Profiling of high molecular weight esters by flow injection analysis-high resolution mass spectrometry for the characterization of raw and archaeological beeswax and resinous substances, Talanta 212 (2020)

120800. doi:10.1016/j.talanta.2020.120800.
URL https://linkinghub.elsevier.com/retrieve/pii/S0039914020300916

[33] J. La Nasa, M. Zanaboni, D. Uldanck, I. Degano, F. Modugno, H. Kutzke, E. S. Tveit, B. Topalova-Casadiego, M. P. Colombini, Novel application of liquid chromatography/mass spectrometry for the characterization of drying oils in art: Elucidation on the composition of original paint materials used by Edvard Munch (1863–1944), Analytica Chimica Acta 896 (2015) 177–189. doi:10.1016/j.aca.2015.09.023.
URL https://linkinghub.elsevier.com/retrieve/pii/S0003267015011629

[34] M. Cotte, V. Gonzalez, F. Vanmeert, L. Monico, C. Dejoie, M. Burghammer, L. Huder, W. de Nolf, S. Fisher, I. Fazlic, C. Chauffeton, G. Wallez, N. Jiménez, F. Albert-Tortosa, N. Salvadó, E. Possenti, C. Colombo, M. Ghirardello, D. Comelli, E. Avranovich Clerici, R. Vivani, A. Romani, C. Costantino, K. Janssens, Y. Taniguchi, J. McCarthy, H. Reichert, J. Susini, The "Historical Materials BAG": A New Facilitated Access to Synchrotron X-ray Diffraction Analyses for Cultural Heritage Materials at the European Synchrotron Radiation Facility, Molecules 27 (6) (2022) 1997. doi:10.3390/molecules27061997.
URL https://www.mdpi.com/1420-3049/27/6/1997

[35] R. Gid, Raymond Gid: affichiste et typographe, no. 2 in Collection Affichistes, Mairie de Paris, Agence culturelle de Paris, Paris, 1992.

[36] Z. Oyman, W. Ming, R. van der Linde, Oxidation of drying oils containing non-conjugated and conjugated double bonds catalyzed by a cobalt catalyst, Progress in Organic Coatings 54 (3) (2005) 198–204. doi:10.1016/j.porgcoat.2005.06.004.
URL https://linkinghub.elsevier.com/retrieve/pii/S030094400500144X

[37] W. Muizebelt, J. Hubert, R. Venderbosch, Mechanistic study of drying of alkyd resins using ethyl linoleate as a model substance, Progress in Organic Coatings 24 (1-4) (1994) 263–279. doi:10.1016/0033-0655(94)85019-4.
URL https://linkinghub.elsevier.com/retrieve/pii/0033065594850194

[38] R. Mayer, S. Sheehan, The artist's handbook of materials and techniques, fifth edition, revised and expanded Edition, Faber and Faber, London, 1991, 978-0-571-15067-0.

[39] P. Helou de la Grandière, Recherche sur le rôle des savons metalliques dans le développement des clivages des peintures de Pierre Soulages de 1959, Tech. rep., Centre national des Arts Plastiques, France, Paris (2008).
URL http://rgdoi.net/10.13140/2.1.1961.5528

[40] H. A. L. Standeven, Oil-Based House Paints from 1900 to 1960: An Examination of Their History and Development, with Particular Reference to Ripolin Enamels, Journal of the American Institute for Conservation 52 (3) (2013) 127–139. doi:10.1179/1945233013Y.0000000006.
URL http://www.tandfonline.com/doi/full/10.1179/1945233013Y.0000000006

[41] R. Mazzeo, S. Prati, M. Quaranta, E. Joseph, E. Kendix, M. Galeotti, Attenuated total reflection micro FTIR characterisation of pigment-binder interaction in reconstructed paint films, Analytical

and Bioanalytical Chemistry 392 (1-2) (2008) 65–76. doi:10.1007/s00216-008-2126-5.
URL http://link.springer.com/10.1007/s00216-008-2126-5

[42] L. de Viguerie, P. Payard, E. Portero, P. Walter, M. Cotte, The drying of linseed oil investigated by Fourier transform infrared spectroscopy: Historical recipes and influence of lead compounds, Progress in Organic Coatings 93 (2016) 46–60. doi:10.1016/j.porgcoat.2015.12.010.
URL https://linkinghub.elsevier.com/retrieve/pii/S0300944015303878

[43] J. van der Weerd, A. van Loon, J. J. Boon, FTIR Studies of the Effects of Pigments on the Aging of Oil, Studies in Conservation 50 (1) (2005) 3–22. doi:10.1179/sic.2005.50.1.3.
URL http://www.tandfonline.com/doi/full/10.1179/sic.2005.50.1.3

[44] R. J. Meilunas, J. G. Bentsen, A. Steinberg, Analysis of aged paint binders by FTIR spectroscopy, Studies in Conservation 35 (1) (1990) 33–51. doi:10.1179/sic.1990.35.1.33.
URL http://www.tandfonline.com/doi/full/10.1179/sic.1990.35.1.33

[45] M. Lazzari, O. Chiantore, Drying and oxidative degradation of linseed oil, Polymer Degradation and Stability 65 (2) (1999) 303–313. doi:10.1016/S0141-3910(99)00020-8.
URL https://linkinghub.elsevier.com/retrieve/pii/S0141391099000208

[46] J. Mallégol, J.-L. Gardette, J. Lemaire, Long-term behavior of oil-based varnishes and paints I. Spectroscopic analysis of curing drying oils, Journal of the American Oil Chemists' Society 76 (8) (1999) 967–976. doi:10.1007/s11746-999-0114-3.
URL http://doi.wiley.com/10.1007/s11746-999-0114-3

[47] L. Monico, F. Rosi, C. Miliani, A. Daveri, B. G. Brunetti, Non-invasive identification of metal-oxalate complexes on polychrome artwork surfaces by reflection mid-infrared spectroscopy, Spectrochimica Acta Part A: Molecular and Biomolecular Spectroscopy 116 (2013) 270–280. doi:10.1016/j.saa.2013.06.084.
URL https://linkinghub.elsevier.com/retrieve/pii/S1386142513006884

[48] S. Bruni, F. Cariati, F. Casadio, L. Toniolo, Spectrochemical characterization by micro-FTIR spectroscopy of blue pigments in different polychrome works of art, Vibrational Spectroscopy 20 (1) (1999) 15–25. doi:10.1016/S0924-2031(98)00096-4.
URL https://linkinghub.elsevier.com/retrieve/pii/S0924203198000964

[49] H. Stammreich, D. Bassi, O. Sala, H. Siebert, The vibrational spectrum of the dichromate ion, Spectrochimica Acta 13 (3) (1958) 192–196. doi:10.1016/0371-1951(58)80076-4.
URL https://linkinghub.elsevier.com/retrieve/pii/0371195158800764

[50] R. L. Carter, C. E. Bricker, Comparison of the vibrational spectra of K2Cr2O7, Rb2Cr2O7 and CS2Cr2O7, Spectrochimica Acta Part A: Molecular Spectroscopy 29 (2) (1973) 253–262. doi:10.1016/0584-8539(73)80069-8.
URL https://linkinghub.elsevier.com/retrieve/pii/0584853973800698

[51] F. C. Izzo, M. Kratter, A. Nevin, E. Zendri, A Critical Review on the Analysis of Metal Soaps in Oil Paintings, ChemistryOpen 10 (9) (2021) 904–921. doi:10.1002/open.202100166.

URL https://chemistry-europe.onlinelibrary.wiley.com/doi/10.1002/open.202100166

[52] K. J. van den Berg, A. Burnstock, M. Schilling, Notes on Metal Soap Extenders in Modern Oil Paints: History, Use, Degradation, and Analysis, in: F. Casadio, K. Keune, P. Noble, A. Van Loon, E. Hendriks, S. A. Centeno, G. Osmond (Eds.), Metal Soaps in Art, Springer International Publishing, Cham, 2019, pp. 329–342, series Title: Cultural Heritage Science 978-3-319-90617-1. doi:10.1007/978-3-319-90617-1_19.
URL http://link.springer.com/10.1007/978-3-319-90617-1_19

[53] I. Fiedler, M. A. Bayard, Cadmium Yellows, Oranges and Reds, in: Artists' Pigments, A Handbook of their History and Characteristics, Vol. 1, National Gallery of Art; Archetype Publications, Washington; London, 1986, pp. 65–108.

[54] L. Monico, L. Cartechini, F. Rosi, A. Chieli, C. Grazia, S. De Meyer, G. Nuyts, F. Vanmeert, K. Janssens, M. Cotte, W. De Nolf, G. Falkenberg, I. C. A. Sandu, E. S. Tveit, J. Mass, R. P. de Freitas, A. Romani, C. Miliani, Probing the chemistry of CdS paints in *The Scream* by in situ noninvasive spectroscopies and synchrotron radiation x-ray techniques, Science Advances 6 (20) (2020) eaay3514. doi:10.1126/sciadv.aay3514.
URL https://www.science.org/doi/10.1126/sciadv.aay3514

[55] G. Van der Snickt, J. Dik, M. Cotte, K. Janssens, J. Jaroszewicz, W. De Nolf, J. Groenewegen, L. van der Loeff, Characterization of a Degraded Cadmium Yellow (CdS) Pigment in an Oil Painting by Means of Synchrotron Radiation Based X-ray Techniques, Analytical Chemistry 81 (7) (2009) 2600–2610. doi:10.1021/ac802518z.
URL https://pubs.acs.org/doi/10.1021/ac802518z